Geometric phases and competing orders in two dimensions

Liang Fu and Subir Sachdev

Department of Physics, Harvard University, Cambridge MA 02138

Cenke Xu

Department of Physics, University of California, Santa Barbara CA 93106

(Dated: October 20, 2010)

Abstract

We discuss the problem of characterizing "quantum disordered" ground states, obtained upon loss of antiferromagnetic order on general lattices in two spatial dimensions, with arbitrary electronic band structure. A key result is the response in electron bilinears to the skyrmion density in the local antiferromagnetic order, induced by geometric phases. We also discuss the connection to topological terms obtained under situations where the electronic spectrum has a Dirac form.

I. INTRODUCTION

Geometric phases have played a central role in many fields of physics, and especially in the quantum Hall effect at high magnetic fields[1]. However, in subsequent research it has also become clear that geometric phases are crucial for a complete understanding of the quantum phase transitions of correlated electron systems in zero applied magnetic field. Traditionally, classical phase transitions are described in terms of an 'order parameter', with one phase being ordered, and the other 'disordered'. Upon extending this idea to quantum phase transitions, we have the possibility of a 'quantum-disordered' phase[2]. However, in almost all of the interesting examples, the latter phase is not disordered: geometric phases induce a 'competing' order. A separate possibility is that the quantum-disordered phase has fractionalization and topological order: we will not explore this latter possibility in the present paper.

(We note here that the word 'phase' has two separate meanings above, and in the remainder of the paper. When used by itself, 'phase' refers to a particular state of a thermodynamic system. However, in the combination 'geometric phase', it refers to the angular co-ordinate of a complex number representing the wavefunction. We trust the context will clarify the meaning for the reader.)

In two dimensional systems, the earliest example of a competing order induced by geometric phases was in the spin $S = 1/2$ square lattice Heisenberg antiferromagnet. The model with nearest-neighbor interactions has long-range Néel order. We can try to destroy this order by adding further neighbor frustrating interactions, leading to a possible quantum-disordered phase[2]. Such a phase should be characterized by the proliferation of defects in the Néel order: for collinear Néel order in a model with SU(2) spin symmetry, the order parameter lies on S^2 (the surface of a sphere), and the homotopy group $\pi_2(S^2) = Z$, implies that the existence of point defects known as hedgehogs. Haldane[3] pointed out that geometric phases of the lattice spins endowed each hedgehog with a net geometric phase, and argued that this implied a 4-fold degeneracy of the quantum-disordered ground state. Read and Sachdev[4,5] demonstrated that the hedgehog geometric phase actually implied a competing order, associated with a broken lattice symmetry due to valence bond solid (VBS) order. The VBS order can take 4 orientations related by lattice symmetries, thus realizing the 4-fold degeneracy. They also presented two additional derivations of the hedgehog geometric phase: from the Schwinger boson representation of the spins[5], and via a duality transform of the quantum dimer model[6]. Sachdev and Jalabert[7] introduced a lattice gauge theory for the competing Néel and VBS orders, in which the geometric phase appeared as a coupling between the skyrmion density associated with the Néel order (defined in Section II) and a lattice field linked to the VBS order.

We note in passing that we will not be interested here on the separate question of the nature of the phase transition between the two competing order phases. A second order transition appears in the 'deconfined criticality' theory[8,9], and this proposal has been the

focus of a number of numerical studies[10–17].

A different perspective on the Néel-VBS transition appeared in the work of Tanaka and Hu[18] who used a continuum theory of Dirac fermions. The previous works had all represented the spins in terms of bosonic degrees of freedom which carried geometric phases. Tanaka and Hu instead used a fermionic representation of the spins, and then chose a low-energy limit which allowed representation of the theory in terms of continuum Dirac fermions in 2+1 spacetime dimensions. The Dirac representation appeared from a band structure of the lattice fermions in which there was π flux per plaquette: this could be interpreted as the dispersion of fermionic spinons in a a particular algebraic spin liquid (ASL) important for intermediate length-scale physics, or as a mean-field dispersion of electrons in a particular extended Hubbard model[20]. Armed with the Dirac fermions, Tanaka and Hu used field-theoretic developments by Abanov and Wiegmann[19] to show that the effective action for the Néel and VBS order parameters allowed representation of the geometric phase as a Wess-Zumino-Witten (WZW) term for a 5-component order parameter. The co-efficient of this WZW term was quantized to a value reduced consistently to the hedgehog Berry phases in the appropriate limit. In a different context, Grover and Senthil[22] recently showed that a WZW term was also present between a quantum spin Hall order parameter and s-wave superconducting order on the honeycomb lattice; their computation also used the Dirac spectrum of the electrons on the honeycomb lattice.

The appearance of the WZW term with quantized co-efficient in the above computation appears surprising from the perspective of the earlier bosonic formulations[3–5]. In these earlier works, the quantization was directly related to the quantization of the spin on each lattice site, which relied crucially on the projection to one electron (in general, to $2S$ electrons in a fully antisymmetric orbital state, for spin S) on every site. In contrast, in the above fermionic formulations[18,20,22], the local constraints are ignored in the computation of the WZW term, apart from a global constraint on the average fermion density. We will argue in this paper that the WZW term with a quantized co-efficient is an artifact of the low energy Dirac fermionic spectrum.

This aim of our paper is extend the use of the fermionic representation of the underlying degrees of freedom to cases without a low energy Dirac limit. We will develop a general approach to computing geometric phases, which works for arbitrary electronic band structures, whether insulating, metallic or superconducting. Like the recent work[18,20,22], we will not impose a local constraint on the electron number, which is permissible for the metallic or superconducting cases or even in insulators with small on-site repulsive energy. Our computation begins by applying local antiferromagnetic order, and computing the band structure in the presence of this order. Then, we allow the orientation of the local order to become spacetime-dependent, so that eventually there is no true long-range antiferromagnetic order. However, the local ordering is still assumed to be present, with its associated band structure, and we fill these electronic states up to the Fermi level. We will then compute response of these filled electronic states to spatial variations in the antiferromagnetic order. We will also

allow spatial variations in competing orders, deduce their coupling to antiferromagnetism. We will find geometric phases between the order parameters, but will show that a WZW representation does not exist in general.

Another approach to the general problem of geometric phases was described recently by Yao and Lee[23]. Their method required extension[24] of the 2 dimensional electronic band structure to 6 dimensions, and the computation of topological invariants in 6 dimensions and of the mapping between 2 and 6 dimensions. Non-zero values of these invariants were then argued to be sufficient conditions for a WZW term in the effective action for the competing orders. This last conclusion appears to be at variance with our results.

We begin in Section II by considering spatial variations in the antiferromagnetic order on the square lattice. We compute the response to this spatially varying background, in the spirit of the computation of Chern numbers of integer quantum Hall states by Thouless *et al.*[25]. This leads to the key result in Eq. (2.22).

Section III extends the computation to allow for simultaneous variation of both Néel and VBS orders. Here we will also make a connection to the dimensional reduction method[23,24] noted above. Section IV contains applications of our results to insulators on the honeycomb lattice, while Section V considers transitions in the background of the nodal quasiparticles of a d-wave superconductor.

II. FLUCTUATING NÉEL ORDER

Our approach begins with with an arbitrary band structure for lattice fermions c_α, with the spin index $\alpha = \uparrow, \downarrow$; so the band structure of the electronic quasiparticles is

$$H_b = -\sum_{i,j} t(\mathbf{r}_i - \mathbf{r}_j) c_\alpha^\dagger(\mathbf{r}_i) c_\alpha(\mathbf{r}_j) \tag{2.1}$$

where $\mathbf{r}_i$ labels the lattice sites, and $t(\mathbf{r})$ are the tight-binding hopping matrix elements. For definiteness, let us consider the Néel state on the square lattice, as described by the Slater mean-field theory of antiferromagnetic order. We allow the Néel order to have a slow spatial variation in its orientation, which we specify by the unit vector $n^a(\mathbf{r})$ ($a = x, y, z$). In this modulated Néel state, the electronic quasiparticle Hamiltonian is modified from the band structure in Eq. (2.1) to

$$H = -\sum_{i,j} t(\mathbf{r}_i - \mathbf{r}_j) c_\alpha^\dagger(\mathbf{r}_i) c_\alpha(\mathbf{r}_j) + m \sum_i \eta_i n^a(\mathbf{r}_i) c_\alpha^\dagger(\mathbf{r}_i) \sigma_{\alpha\beta}^a c_\beta(\mathbf{r}_i) \tag{2.2}$$

where σ^a are the spin Pauli matrices, $\eta_i = \pm 1$ on the two sublattices of the Néel order, and m is a mean-field magnitude of the band splitting due to the Néel order. The main result of the following Section II A will be obtained by working directly with Eq. (2.2) for a slow variation of $n^a(\mathbf{r})$ about a fully polarized Néel state.

For some purposes, we will find it advantageous to use an alternative gauge-theoretic formulation, which has some technical advantages for a global perspective on the phase diagram. For this, we follow Ref. 26, and transform to a rotating reference frame in the varying Néel background so that the Néel order points in the constant direction (0,0,1) in the new reference frame. We do this by introducing complex bosonic spinors $z_{i\alpha}$, with $|z_{i\uparrow}|^2 + |z_{i\downarrow}|^2 = 1$ so that

$$\begin{pmatrix} c_\uparrow \\ c_\downarrow \end{pmatrix} = \begin{pmatrix} z_\uparrow & -z_\downarrow^* \\ z_\downarrow & z_\uparrow^* \end{pmatrix} \begin{pmatrix} \psi_+ \\ \psi_- \end{pmatrix} \tag{2.3}$$

where ψ_p, $p = \pm$, are the "electrons" in the rotating reference frame. We will assume that the z_α have a slow dependence upon spacetime, allowing in expansion in gradients of the z_α. A fixed orientation of the Néel order is realized in the rotating reference frame by choosing the z_α so that

$$n^a = z_\alpha^* \sigma_{\alpha\beta}^a z_\beta \tag{2.4}$$

However, we will *not* assume any slow variations in the fermions c_α and ψ_p, allowing them to carry arbitrary momenta and band structures.

Parameterizations like (2.3) were motivated earlier by the Schwinger boson formulation of the underlying antiferromagnet. In such theories, the geometric phases of the spins at half-filling were associated entirely with those of the Schwinger bosons[5]. In our computations of geometric phases in the present paper, we will find it convenient to work in an approach in which the lattice geometric phases are attached entirely to fermionic degrees of freedom. For this, we will use an exact rotor model formulation of a general lattice Hamiltonian for which Eq. (2.3) also holds. The details of this rotor formulation are presented in Appendix A, and this should be regarded as an alternative to earlier Schwinger boson formulations. In the rotor theory, the $\psi_\pm$ are canonical fermions with a density equal to the full electron density; thus in the the insulator, the total $\psi_\pm$ density is 1, and it is this unit density which leads to the geometric phases. The bosonic variables z_α have a rotor kinetic energy with only a second-order time-derivative in the action *i.e.* they are not canonical bosons, and do not directly carry any geometric phases. In the Schwinger boson formulation, the bosons are canonical, and this complicates the computation of geometric phases in the general case.

Inserting Eq. (2.3) into Eq. (2.2), we obtain the theory for the $\psi_\pm$ fermions, which we write in the form[26]

$$H = -\sum_{i,j} t(\mathbf{r}_i - \mathbf{r}_j) \psi_p^\dagger(\mathbf{r}_i) e^{ipA_{ij}} \psi_p(\mathbf{r}_j) + m \sum_i \eta_i \, p \, \psi_p^\dagger(\mathbf{r}_i) \psi_p(\mathbf{r}_i) + \dots \tag{2.5}$$

First, note that the transformation to the rotating reference frame has removed the slowly varying r dependence from the second term proportional to m. Instead the effect of the transformation into the rotating reference is now entirely in the hopping term. As discussed in earlier work[26], these modifications can be expressed in general in terms of a SU(2) gauge

potential, corresponding to the SU(2) gauge redundancy introduced by the parameterization in Eq. (2.3). In the fluctuating Néel state we consider here, the SU(2) gauge invariance is 'Higgsed' down to U(1): this corresponds to the invariance of Eq. (2.4) only under a U(1) gauge transformation of the z_α. So we write only the U(1) gauge potential term in Eq. (2.5), represented by A_{ij}. The ellipses in Eq. (2.5) refer to additional fermion hopping terms connected to the remaining SU(2) gauge fields: these were written out explicitly in Refs. 26,27, and also appear in the present paper as the last two terms in Eq. (A21).

As we are using a continuum formulation for the order parameter $n^a(\mathbf{r})$ and the z_α, we should also work with a continuum U(1) gauge potential $\mathbf{A}(\mathbf{r})$. This is related to A_{ij} by an integral on straight line between $\mathbf{r}_i$ and $\mathbf{r}_j$

$$A_{ij} = \int_0^1 du\, \mathbf{A}\left(\mathbf{r}_i + u(\mathbf{r}_j - \mathbf{r}_i)\right) \cdot (\mathbf{r}_j - \mathbf{r}_i) \tag{2.6}$$

The flux in the continuum gauge field $\mathbf{A}$ can be related to the 'skyrmion density' in the antiferromagnetic order parameter:

$$\partial_x A_y - \partial_y A_x = \frac{1}{2}\epsilon_{abc} n^a \partial_x n^b \partial_y n^c. \tag{2.7}$$

With periodic boundary conditions, the spatial integral of the skyrmion density on the right-hand-side is a topological invariant, and is quantized to an integer multiple of 2π; the integer is the skyrmion number. Thus inducing a 2π flux in $\mathbf{A}$ corresponds to changing the skyrmion number of the field $n^a(\mathbf{r})$ by unity, which is the same as introducing a hedgehog defect in the Néel order.

A. Response to spin textures

This section will carry out the formally simple exercise of computing the linear response of the Hamiltonian Eq. (2.2) a slowly varying spacetime dependence in the order parameter $n^a(\mathbf{r})$. A similar computation can also be carried out using the alternative gauge-theoretic form in Eq. (2.5) to a slowly varying gauge potential A_{ij}: the latter computation is presented in Appendix B.

We begin with the Hamiltonian in Eq. (2.2), and assume $n^a(\mathbf{r})$ is a slowly varying unit vector. In any local region, without loss of generality, we can choose co-ordinates so that $n^a(\mathbf{r})$ is close to the North pole $(0,0,1)$. In this co-ordinate system, as in Ref. 27, we parameterize the variations in the Néel order in terms of the complex field φ via

$$n^a = \left(\frac{\varphi + \varphi^*}{2}, \frac{\varphi - \varphi^*}{2i}, \sqrt{1 - |\varphi|^2}\right). \tag{2.8}$$

We assume $|\varphi| \ll 1$ and slowly varying. Inserting Eq. (2.8) into Eq. (2.2) we obtain the

Hamiltonian $H = H_0 + H_1$ with

$$H_0 = \sum_{\mathbf{k}} \left(\varepsilon_{\mathbf{k}} c^\dagger(\mathbf{k}) c(\mathbf{k}) + m c^\dagger(\mathbf{k} + \mathbf{Q}) \sigma^z c(\mathbf{k}) \right), \tag{2.9}$$

where $\mathbf{Q} = (\pi, \pi)$ and

$$\varepsilon_{\mathbf{k}} = -\sum_{\mathbf{s}} t(\mathbf{s}) \cos(\mathbf{k} \cdot \mathbf{s}), \tag{2.10}$$

with $t(-\mathbf{s}) = t(\mathbf{s})$. Throughout this section, the summation over momenta extends over the entire square lattice Brillouin zone. Also, we will drop the α spin indices of the c_α, all Pauli matrices in this present section will be assumed to act on the α space, and the α indices will be traced over. The coupling to the spatial variations in the Néel order parameterized by φ are given to the needed order in φ by

$$\begin{aligned} H_1 = {} & m \sum_{\mathbf{k}_1, \mathbf{k}_2} \left[\varphi^*(\mathbf{k}_1) c^\dagger(\mathbf{k}_2 + \mathbf{Q}) \sigma^+ c(\mathbf{k}_2 + \mathbf{k}_1) + \varphi(\mathbf{k}_1) c^\dagger(\mathbf{k}_2 + \mathbf{Q}) \sigma^- c(\mathbf{k}_2 - \mathbf{k}_1) \right] \\ & - \frac{m}{2} \sum_{\mathbf{k}_1, \mathbf{k}_2, \mathbf{k}_3} \varphi^*(\mathbf{k}_1) \varphi(\mathbf{k}_1 + \mathbf{k}_2) c^\dagger(\mathbf{k}_3 + \mathbf{Q}) \sigma^z c(\mathbf{k}_3 - \mathbf{k}_1) \end{aligned} \tag{2.11}$$

We are now interesting in computing the response of the observable properties of H to a slow variation in the Néel order $n^a(\mathbf{r})$. A key choice we have to make here is that of a suitable observable. We are interested in the nature of the phase where Néel order is 'disordered' and so it is natural that the observable should be spin rotation invariant. Also, because we will use the observable to characterize a 'competing order', it should preferably vanish in the spatially uniform Néel state, and be induced only when there are spatial variations in the Néel order. Finally, for convenience, the observable should be a fermion bilinear. With these constraints, it turns out that a unique choice is forced upon us: it is the observable

$$\mathcal{O}(\mathbf{k}, \mathbf{r}) = \int_q \left\langle c^\dagger(\mathbf{k} + \mathbf{Q} + \mathbf{q}/2) c(\mathbf{k} - \mathbf{q}/2) \right\rangle e^{-i\mathbf{q} \cdot \mathbf{r}} \tag{2.12}$$

Here the integral over $\mathbf{q}$ is over *small* momenta, characteristic of those carried by the bosonic fields; thus the variation of $\mathcal{O}(\mathbf{k}, \mathbf{r})$ with $\mathbf{r}$ is slow. In the simplest case, the right-hand-side has support only at $\mathbf{q} = 0$, so that $\mathcal{O}(\mathbf{k}, \mathbf{r})$ takes the $\mathbf{r}$-independent value

$$\mathcal{O}(\mathbf{k}) = \left\langle c^\dagger(\mathbf{k} + \mathbf{Q}) c(\mathbf{k}) \right\rangle. \tag{2.13}$$

On the other hand, $\mathbf{k}$ is an arbitrary momentum in the Brillouin zone, and we will find very useful information in the $\mathbf{k}$ dependence of $\mathcal{O}(\mathbf{k})$. It is easy to check from H_0 that $\mathcal{O}(\mathbf{k}) = 0$ in the uniform Néel state, as we required; only $\left\langle c^\dagger(\mathbf{k} + \mathbf{Q}) \sigma^z c(\mathbf{k}) \right\rangle \neq 0$ in the uniform Néel state. We present an alternative derivation of the choice of the observable $\mathcal{O}$ in Appendix B: there we consider an arbitrary fermion bilinear, and show that it is $\mathcal{O}$ which is uniquely

induced to leading order in the applied gauge flux.

We now proceed to a computation of $\mathcal{O}(\mathbf{k}, \mathbf{r})$ in powers of φ using the Hamiltonian $H_0 + H_1$. We will need to work to second order in φ, and also to second order in spatial gradients of φ; as stated earlier, all fermion momenta are allowed to be arbitrary at all stages.

First, let us collect the propagators of H_0. The single fermion Green's function of H_0 is written in terms of its 'normal' and 'anomalous' parts as

$$
\begin{aligned}
\langle c(\mathbf{k}) \, ; \, c^\dagger(\mathbf{p}) \rangle &= \delta_{\mathbf{k},\mathbf{p}} G(\mathbf{k}) + \delta_{\mathbf{k}+\mathbf{Q},\mathbf{p}} \sigma^z F(\mathbf{k}) \\
G(\mathbf{k}) &\equiv \frac{u_\mathbf{k}^2}{-i\omega + E_{1\mathbf{k}}} + \frac{v_\mathbf{k}^2}{-i\omega + E_{2\mathbf{k}}} \\
F(\mathbf{k}) &\equiv u_\mathbf{k} v_\mathbf{k} \left(\frac{1}{-i\omega + E_{1\mathbf{k}}} - \frac{1}{-i\omega + E_{2\mathbf{k}}} \right),
\end{aligned} \tag{2.14}
$$

where $\mathbf{k}$ takes all values in the square lattice Brillouin zone. The eigenenergies in Eq. (2.14) are

$$
E_{1,2\mathbf{k}} = \frac{\varepsilon_\mathbf{k} + \varepsilon_{\mathbf{k}+\mathbf{Q}}}{2} \pm \sqrt{\left(\frac{\varepsilon_\mathbf{k} - \varepsilon_{\mathbf{k}+\mathbf{Q}}}{2} \right)^2 + m^2}, \tag{2.15}
$$

and the parameters are

$$
u_\mathbf{k} = \cos(\theta_\mathbf{k}/2) \quad, \quad v_\mathbf{k} = \sin(\theta_\mathbf{k}/2) \tag{2.16}
$$

with

$$
\tan \theta_\mathbf{k} = \frac{m}{(\varepsilon_\mathbf{k} - \varepsilon_{\mathbf{k}+\mathbf{Q}})/2} \quad, \quad 0 < \theta_\mathbf{k} < \pi \tag{2.17}
$$

Note that these relations imply

$$
u_{\mathbf{k}+\mathbf{Q}} = v_\mathbf{k} \quad, \quad v_{\mathbf{k}+\mathbf{Q}} = u_\mathbf{k} \quad, \quad E_{1,\mathbf{k}+\mathbf{Q}} = E_{1\mathbf{k}} \quad, \quad E_{2,\mathbf{k}+\mathbf{Q}} = E_{2\mathbf{k}}. \tag{2.18}
$$

The contributions to $\langle c^\dagger(\mathbf{k}+\mathbf{Q}+\mathbf{q}/2)c(\mathbf{k}-\mathbf{q}/2) \rangle$ to second order in φ are shown in Fig. 1. The last diagram vanishes identically, while the first two evaluate to

$$
\langle c^\dagger(\mathbf{k} + \mathbf{Q})c(\mathbf{k} + \mathbf{q}_1 - \mathbf{q}_2) \rangle = \sum_{\mathbf{q}_1,\mathbf{q}_2} J(\mathbf{k}, \mathbf{q}_1, \mathbf{q}_2) \varphi^*(\mathbf{q}_2) \varphi(\mathbf{q}_1) \tag{2.19}
$$

where

$$
\begin{aligned}
J(\mathbf{k}, \mathbf{q}_1, \mathbf{q}_2) = m^2 \sum_\omega \Big[&F(\mathbf{k})G(\mathbf{k} + \mathbf{Q} - \mathbf{q}_2)G(\mathbf{k} + \mathbf{q}_1 - \mathbf{q}_2) \\
- \ &G(\mathbf{k} + \mathbf{Q})F(\mathbf{k} - \mathbf{q}_2)G(\mathbf{k} + \mathbf{q}_1 - \mathbf{q}_2) + G(\mathbf{k} + \mathbf{Q})G(\mathbf{k} - \mathbf{q}_2)F(\mathbf{k} + \mathbf{q}_1 - \mathbf{q}_2) \\
- \ &F(\mathbf{k})F(\mathbf{k} - \mathbf{q}_2)F(\mathbf{k} + \mathbf{q}_1 - \mathbf{q}_2) \Big] - (\mathbf{q}_1 \leftrightarrow -\mathbf{q}_2) \tag{2.20}
\end{aligned}
$$
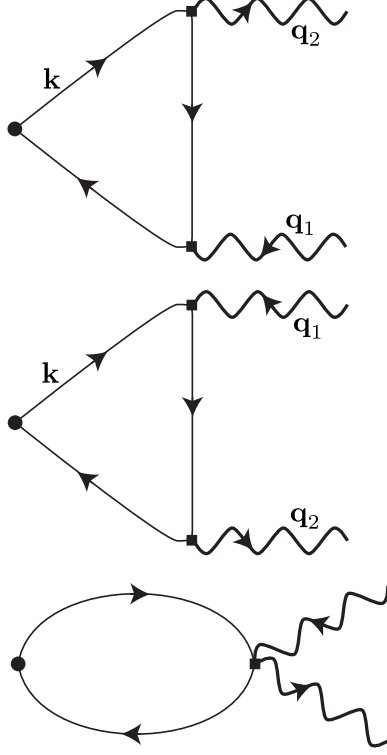
8

FIG. 1: Diagrammatic perturbation theory for $\mathcal{O}$ using the couplings in H_1 in Eq. (2.11). The wavy lines are φ sources, the filled circle is the $\mathcal{O}$ source, while the full lines are c propagators.

We now expand this to second order in $\mathbf{q}_1$ and $\mathbf{q}_2$. This leads to very lengthy expressions, which we simplified using Mathematica. In the end, a simple final result was obtained:

$$J(\mathbf{k}, \mathbf{q}_1, \mathbf{q}_2) = (\mathbf{q}_1 \times \mathbf{q}_2) \left(\frac{\partial \varepsilon_{\mathbf{k}+\mathbf{Q}}}{\partial \mathbf{k}} \times \frac{\partial \varepsilon_{\mathbf{k}}}{\partial \mathbf{k}} \right) \sum_\omega \frac{m^3}{(-i\omega + E_{1\mathbf{k}})^3 (-i\omega + E_{2\mathbf{k}})^3} \qquad (2.21)$$

Now we combine Eqs. (2.19) and (2.21). The Fourier transform of $(\mathbf{q}_1 \times \mathbf{q}_2)\varphi^*(\mathbf{q}_2)\varphi(\mathbf{q}_1)$ is $\partial_x\varphi\partial_y\varphi^* - \partial_y\varphi\partial_x\varphi^*$ and to second order in φ this equals $-2i(\partial_x n^x \partial_y n^y - \partial_x n^y \partial_y n^x)$. In a spin rotationally invariant form, this expression is proportional to the skyrmion density, and so we have one of our main results:

$$\mathcal{O}(\mathbf{k}, \mathbf{r}) = -i\mathcal{F}(\mathbf{k})\epsilon_{abc}n^a(\mathbf{r})\partial_x n^b(\mathbf{r})\partial_y n^c(\mathbf{r}) \qquad (2.22)$$

where

$$\begin{aligned}
\mathcal{F}(\mathbf{k}) &= \left(\frac{\partial \varepsilon_{\mathbf{k}+\mathbf{Q}}}{\partial \mathbf{k}} \times \frac{\partial \varepsilon_{\mathbf{k}}}{\partial \mathbf{k}} \right) \sum_\omega \frac{2m^3}{(-i\omega + E_{1\mathbf{k}})^3 (-i\omega + E_{2\mathbf{k}})^3} \\
&= 6m^3 \left(\frac{\partial \varepsilon_{\mathbf{k}+\mathbf{Q}}}{\partial \mathbf{k}} \times \frac{\partial \varepsilon_{\mathbf{k}}}{\partial \mathbf{k}} \right) \frac{(\mathrm{sgn}(E_{1\mathbf{k}}) - \mathrm{sgn}(E_{2\mathbf{k}}))}{(E_{1\mathbf{k}} - E_{2\mathbf{k}})^5}.
\end{aligned} \qquad (2.23)$$

In the last step, we have evaluated frequency summation at zero temperature. In the re-

9

maining analysis we will assume we are dealing with a fully gapped insulator with $E_{1\mathbf{k}} > 0$ and $E_{2\mathbf{k}} < 0$ over the entire Brillouin zone. The metallic case has singularities at the Fermi surfaces which are at $E_{1\mathbf{k}} = 0$ or $E_{2\mathbf{k}} = 0$, but we will not explore its consequences here; indeed in our expansion in powers of $\mathbf{q}_{1,2}$, we have implicitly assumed smooth behavior across the Brillouin zone. Note that in both the insulator and the metal there is no singularity due to the denomination in Eq. (2.23): via Eq. (2.15) we always have $E_{1\mathbf{k}} - E_{2\mathbf{k}} \geq 2m$.

A plot of $\mathcal{F}(\mathbf{k})$ for the insulating case is shown in Fig. 2.
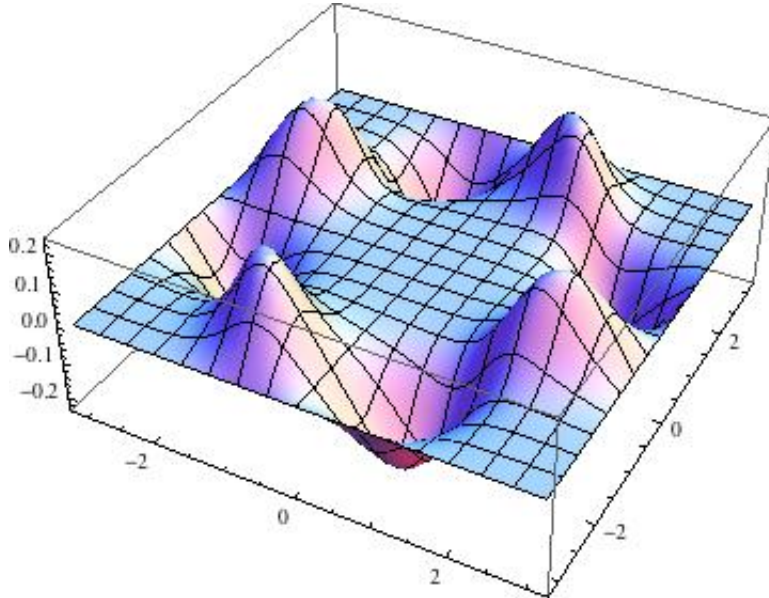

FIG. 2: A plot of the function $\mathcal{F}(\mathbf{k})$ in Eq. (B11) for $\varepsilon_{\mathbf{k}} = \cos k_x - \cos k_y + 0.4 \cos(k_x + k_y) + 0.4 \cos(k_x - k_y)$ and $m = 1$.

The integral of $\mathcal{F}(\mathbf{k})$ is zero over the Brillouin zone. However, note that it has the same symmetry as the function $(\cos k_x - \cos k_y) \sin k_x \sin k_y$; so the integral of $\mathcal{F}(\mathbf{k})(\cos k_x - \cos k_y) \sin k_x \sin k_y$ is non-zero. This suggest we define the charge $\mathcal{Q}$ by

$$\mathcal{Q} = -i \sum_{\mathbf{k}} c^\dagger(\mathbf{k}) c(\mathbf{k} + \mathbf{Q})(\cos k_x - \cos k_y) \sin k_x \sin k_y. \tag{2.24}$$

Note $\mathcal{Q}^\dagger = \mathcal{Q}$.

Our main result in Eq. (2.22) implies that any quantum fluctuation which leads to a non-zero value of the skyrmion density $\epsilon_{abc} n^a \partial_x n^b \partial_y n^c$ will induce a change in $\mathcal{O}$. Generically, a change in $\mathcal{O}$ must imply a corresponding change in $\mathcal{Q}$ because the two observables have identical signatures under all symmetries of the Hamiltonian. In paticular, a hedgehog tunneling event is one in which the spatial integral of $\epsilon_{abc} n^a \partial_x n^b \partial_y n^c$ (the skyrmion number) changes by 4π. Thus, before the hedgehog event $\langle \mathcal{Q} \rangle = 0$, while after the hedgehog tunneling event, we have $\langle \mathcal{Q} \rangle \neq 0$. We can normalize $\mathcal{Q}$ so that $\langle \mathcal{Q} \rangle = 1$ for each hedgehog, and the normalization constant will depend upon Eq. (2.23) and the details on the band structure.

10

Then with such a normalization, we have the important correspondence

$$\mathcal{Q} \cong \text{skyrmion number.} \tag{2.25}$$

This is the key result of the present subsection. We emphasize that such a correspondence is possible because both the skyrmion number and $\mathcal{Q}$ are invariant under spin rotations, have identical transformations under all square lattice space group operations, and are both odd under time-reversal.

B. Connection to VBS order

The results in Eqs. (2.22) and (2.25) suggest strong consequences in the 'quantum disordered' phase where Néel order has been lost. Such a phase will have a proliferation of hedgehog tunnelling events, and so Eq. (2.25) implies that there will be correspondingly large fluctuations in the charge $\mathcal{Q}$. We can therefore expect that fluctuations in variables conjugate to $\mathcal{Q}$ will be suppressed, and will therefore have long-range order: this is the competing order induced by the geometric phase in Eq. (B10). Thus any quantum variable conjugate to $\mathcal{Q}$ is a bona-fide competing order. There are many possibilities, but here, we verify that the traditional VBS order does satisfy the requirements. A more specific field-theoretic discussion of the appearance of VBS order in the quantum-disordered Néel phase will be given in Section III A.

The VBS order is $V = V_x + iV_y$ defined by

$$\begin{aligned}
V_x &= i\sum_{\mathbf{k}} c^\dagger(\mathbf{k})c(\mathbf{k}+\mathbf{Q}_x)\sin k_x \\
V_y &= i\sum_{\mathbf{k}} c^\dagger(\mathbf{k})c(\mathbf{k}+\mathbf{Q}_y)\sin k_y
\end{aligned} \tag{2.26}$$

where $\mathbf{Q}_x = (\pi, 0)$ and $\mathbf{Q}_y = (0, \pi)$. Now we can compute the commutators

$$\begin{aligned}
[\mathcal{Q}, V_x] &= -\sum_{\mathbf{k}} c^\dagger(\mathbf{k})c(\mathbf{k}+\mathbf{Q}_y)\sin k_y \frac{(\cos(k_x) - \cos(3k_x))}{2} \simeq iV_y \\
[\mathcal{Q}, V_y] &= \sum_{\mathbf{k}} c^\dagger(\mathbf{k})c(\mathbf{k}+\mathbf{Q}_x)\sin k_x \frac{(\cos(k_y) - \cos(3k_y))}{2} \simeq -iV_x
\end{aligned} \tag{2.27}$$

Here the $\simeq$ means that the two operators have the same symmetry under the square lattice space group. Thus we have the key result

$$[\mathcal{Q}, V] \simeq V. \tag{2.28}$$

This means that V is a raising order for $\mathcal{Q}$. But, as we noted in Section II A, this is precisely

the effect of the monopole tunneling event: in other words, V has the same quantum numbers as a monopole operator. Then, following the reasoning in Refs. 5,9, we may conclude that V is a competing order which becomes long-range in the quantum-disordered Néel phase.

An alternative route to determining an operator conjugate to $\mathcal{Q}$ is to determine a V so that $-i(V^\dagger \partial_t V - V \partial_t V^\dagger) \simeq \mathcal{Q}$. It is easy to check that the definition in Eq. (2.26) does satisfy the needed requirements. We have the time derivative

$$\frac{dV_x}{dt} = \sum_{\mathbf{k}} \sin k_x (\varepsilon_{\mathbf{k}} - \varepsilon_{\mathbf{k}+\mathbf{Q}_x}) c^\dagger(\mathbf{k}) c(\mathbf{k}+\mathbf{Q}_x) + 2m \sum_{\mathbf{k}} \sin k_x c^\dagger(\mathbf{k}) \sigma^z c(\mathbf{k}+\mathbf{Q}_y) \quad (2.29)$$

and similarly for V_y. For simplicitly, we will drop the terms proportional to m, and work in the limit of small m. So we have

$$-i\left(V_y \frac{dV_x}{dt} - V_x \frac{dV_y}{dt}\right) = \sum_{\mathbf{k},\mathbf{q}} \sin k_x \sin q_y (\varepsilon_{\mathbf{k}} - \varepsilon_{\mathbf{k}+\mathbf{Q}_x}) c^\dagger(\mathbf{q}) c(\mathbf{q}+\mathbf{Q}_y) c^\dagger(\mathbf{k}) c(\mathbf{k}+\mathbf{Q}_x)$$
$$- (x \leftrightarrow y) \quad (2.30)$$

Now we can factorize the 4-Fermi term using $\langle c^\dagger(\mathbf{k}) c(\mathbf{k}) \rangle = n(\mathbf{k})$:

$$-i\left(V_y \frac{dV_x}{dt} - V_x \frac{dV_y}{dt}\right) = \sum_{\mathbf{k}} \sin k_x \sin k_y c^\dagger(\mathbf{k}) c(\mathbf{k}+\mathbf{Q}) \Big[(\varepsilon_{\mathbf{k}+\mathbf{Q}_y} - \varepsilon_{\mathbf{k}+\mathbf{Q}})(1 - n(\mathbf{k}+\mathbf{Q}_y))$$
$$- (\varepsilon_{\mathbf{k}} - \varepsilon_{\mathbf{k}+\mathbf{Q}_x}) n(\mathbf{k}+\mathbf{Q}_x) \Big] - (x \leftrightarrow y)$$
$$= \sum_{\mathbf{k}} \sin k_x \sin k_y c^\dagger(\mathbf{k}) c(\mathbf{k}+\mathbf{Q}) \Big[\varepsilon_{\mathbf{k}+\mathbf{Q}_y} - \varepsilon_{\mathbf{k}+\mathbf{Q}_x}$$
$$+ 2(\varepsilon_{\mathbf{k}+\mathbf{Q}_x} n(\mathbf{k}+\mathbf{Q}_x) - \varepsilon_{\mathbf{k}+\mathbf{Q}_y} n(\mathbf{k}+\mathbf{Q}_y))$$
$$- (\varepsilon_{\mathbf{k}} + \varepsilon_{\mathbf{k}+\mathbf{Q}})(n(\mathbf{k}+\mathbf{Q}_x) - n(\mathbf{k}+\mathbf{Q}_y)) \Big] \quad (2.31)$$

The r.h.s. is indeed $\simeq \mathcal{Q}$.

III.   FLUCTUATING NÉEL AND VBS ORDERS

Given the connection between the skyrmion number of the Néel order and the VBS order derived in Section II, it is natural to wonder whether the two order parameters can be treated at a more equal footing. In Section II we investigated the fermion correlations in the background of a spatially varying Néel order, and so this suggests a natural generalization in which we allow for a background spacetime dependence of *both* the Néel and VBS orders. This section will present the needed generalization. The result here will be an alternative derivation of the arguments of Section II B: the skyrmion number of the Néel order and the angular variable, ϕ, of VBS order $V \sim e^{i\phi}$ are quantum-mechanically conjugate variables.

We start from a Neel state with the order parameter $m^a = m(n^x, n^y, n^z) \neq 0$. When the

system approaches the Neel-VBS transition, fluctuating VBS order becomes important and needs to be taken into account. The starting point of our analysis is the electron Hamiltonian H with both m^a and V:

$$H(V_x, V_y, n^x, n^y) = [H_b + mH_z^N] + [V_x H_x^V + V_y H_y^V + m(n^x H_x^N + n^y H_y^N)] \quad (3.1)$$

where H_b describes the electron band structure in the absence of Neel or VBS order as in Eq. (2.1); the fermion bilinear operator (H_x^V, H_y^V) is dimerized electron hopping in x and y directions; (H_x^N, H_y^N, H_z^N) is staggered electron spin density in x, y, z directions in spin space; (V_x, V_y) describes the fluctuating VBS order; (n^x, n^y) describes the Goldstone mode of the Néel order. We now integrate out the fermions and derive the effective action S for the slowly varying bosonic fields $\mathcal{A}^\mu(x, y, \tau) \equiv (V_x, V_y, n^x, n^y)$.

Treating the second term in H as a perturbation, we find couplings between Neel and VBS order starts at fourth order in a one-loop expansion:

$$S_1 = \sum_{\mu,\nu,\lambda,\delta} \int \prod_{i=1}^{3} d\mathbf{p}_i \, K_{\mathbf{p_1 p_2 p_3}}^{\mu\nu\lambda;\delta} \cdot \mathcal{A}^\mu(\mathbf{p}_1)\mathcal{A}^\nu(\mathbf{p}_2)\mathcal{A}^\lambda(\mathbf{p}_3)\mathcal{A}^\delta(-\mathbf{p}_1 - \mathbf{p}_2 - \mathbf{p}_3), \quad (3.2)$$

[Note: we drop all numerical prefactors in this subsection.] Here $\mu, \nu, \lambda, \delta = 1, ...4$ labels the components of the perturbation field $\mathcal{A}^\mu$ and the vertex; $\mathbf{p} = (p^0, p^x, p^y)$ is the external momenta of $\mathcal{A}^\mu$. We now expand the function K in powers of $\mathbf{p}$ and collect terms involving the product $p_1^\alpha p_2^\beta p_3^\gamma$ with $\alpha, \beta, \gamma = 0, x, y$:

$$K_{\mathbf{p_1 p_2 p_3}}^{\mu\nu\lambda;\delta} = K_{\alpha\beta\gamma}^{\mu\nu\lambda;\delta} \cdot p_1^\alpha p_2^\beta p_3^\gamma + ... \quad (3.3)$$

This corresponds to a derivative expansion in real spacetime:

$$S_1 = \sum_{\mu,\nu,\lambda,\delta} K_{\alpha\beta\gamma}^{\mu\nu\lambda;\delta} \int dx dy d\tau \, (\mathcal{A}^\delta \partial_\alpha \mathcal{A}^\mu \partial_\beta \mathcal{A}^\nu \partial_\gamma \mathcal{A}^\lambda) \quad (3.4)$$

The action (3.4) resembles the Chern-Simons theory in 6+1 dimensions. A difference is that the space-time indices α, β, γ and the internal indices $\mu, \nu, \delta, \lambda$ do not mix with each other. Qi et al.[24] recently proposed that S_1 can be simply obtained from the Chern-Simons term by dimensional reduction to 2+1 dimensions. The procedure is to throw away all components in the Chern-Simons term, which involve spatial derivatives in the internal dimension. We shall show by calculating $K_{\alpha\beta\gamma}^{\mu\nu\lambda;\delta}$ explicitly that this dimensional reduction approach does not apply in the present situation.

Among the terms in S_1, we are particularly interested in a topological term

$$S_{top} = \sum_{\alpha\beta} iK_{\alpha\beta} \int dx dy d\tau \, j_\alpha^N j_\beta^V, \quad (3.5)$$

13

where j_α^N is the skyrmion current in the Neel state:

$$j_\alpha^N \equiv \epsilon_{\alpha\beta\gamma}\epsilon_{abc}n^a\partial_\beta n^b\partial_\gamma n^c, \tag{3.6}$$

and j_β^V is the VBS current:

$$j_\beta^V \equiv V_x\partial_\beta V_y - V_y\partial_\beta V_x. \tag{3.7}$$

It follows from symmetry analysis that on the square and honeycomb lattice, The matrix $K_{\alpha\beta}$ is diagonal. Because of four- and six-fold rotational symmetry, $K_{xx} = K_{yy}$. S_{top} then becomes

$$S_{top} = i \int dxdyd\tau \ (Kj_t^N j_t^V + K'j_x^N j_x^V + K'j_y^N j_y^V), \tag{3.8}$$

Comparing (3.8) and (3.4), we can express K in terms of the tensor components $K_{\alpha\beta\gamma}^{\mu\nu\lambda;\delta}$:

$$\begin{aligned} K \ \propto \ & [K_{0xy}^{234;1} + \text{Permutations of (2,0), (3,x), and (4,y)}] \\ & - [K_{0xy}^{243;1} + \text{Permutations of (2,0), (4,x), and (3,y)}] \\ & - [K_{0xy}^{134;2} + \text{Permutations of (1,0), (3,x), and (4,y)}] \\ & + [K_{0xy}^{143;2} + \text{Permutations of (1,0), (4,x), and (3,y)}] \end{aligned} \tag{3.9}$$

We now calculate K for the square lattice. The Hamiltonian H_b is specified in Eq. (2.1), and we choose only nearest neighbor hopping t. For the coupling to the order parameters, we choose

$$\begin{aligned} H_a^N &= \sum_{i\in A} c^\dagger(\mathbf{r}_i)\sigma^a c(\mathbf{r}_i) - \sum_{i\in B} c^\dagger(\mathbf{r}_i)\sigma^a c(\mathbf{r}_i) \\ H_\beta^V &= \sum_{i\in A}(-1)^{i_\beta}[c^\dagger(\mathbf{r}_i)c(\mathbf{r}_i + \mathbf{e}_\beta) + c.c.], \ \beta = x, y \end{aligned} \tag{3.10}$$

where we have divided the square lattice into two sublattices A and B defined by $(-1)^{i_x+i_y} = \pm 1$. The Néel order carries crystal momentum (π,π). The VBS order in the x- and y-directions carries crystal momentum $(\pi,0)$ and $(0,\pi)$ respectively, with the corresponding dimerization pattern shown in Fig. 3. Note that the dimerization pattern "rotates" around a site as the phase of $V_x + iV_y$ advances by 2π. It is straightforward to check that the term S_{top} in Eq.(3.4) satisfies square lattice symmetry.

The lattice periodicity is doubled in both the x and y direction for $m \neq 0$ and $V_x, V_y \neq 0$. We choose the 4 sites in a plaquette as the new unit cell. The Bloch Hamiltonian $H(k_x, k_y)$
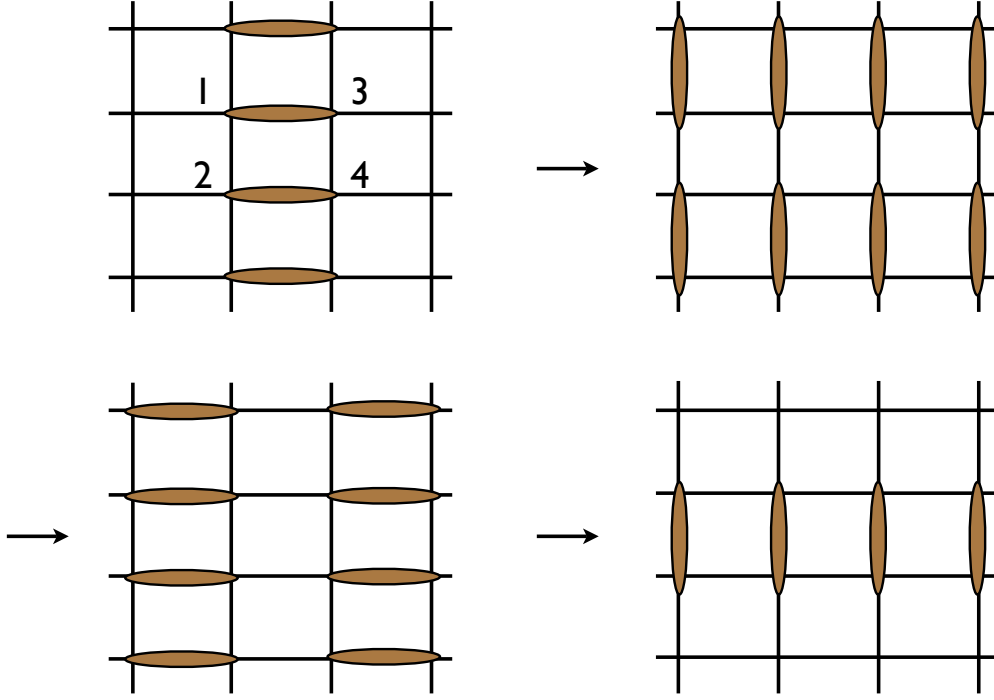
FIG. 3: VBS order on the square lattice.

is obtained by Fourier transform:

$$
H(k_x, k_y) = \begin{pmatrix} m^a \sigma^a & t_y & t_x & 0 \\ t_y^* & -m^a \sigma^a & 0 & t_x \\ t_x^* & 0 & -m^a \sigma^a & t_y \\ 0 & t_x^* & t_y^* & m^a \sigma^a \end{pmatrix}
$$
$$
t_y = -t \cos k_y + i V_y \sin k_y,
$$
$$
t_x = -t \cos k_x + i V_x \sin k_x. \tag{3.11}
$$

Here $k_x, k_y \in [-\pi/2, \pi/2]$ is crystal momentum in the folded Brilluoin zone. We used Mathematica to evaluate K and found

$$
K = \int dk_0 dk_x dk_y \frac{m^3 t^2 \sin^2 k_x \sin^2 k_y [t^4 (\cos^2 k_x - \cos^2 k_y)^2 - (k_0^2 + m^2)^2]}{[t^2 (\cos k_x - \cos k_y)^2 + k_0^2 + m^2]^3 [t^2 (\cos k_x + \cos k_y)^2 + k_0^2 + m^2]^3}. \tag{3.12}
$$

The integration over k_0 can be done analytically using Mathematica. The resulting integrand $\mathcal{K}(k_x, k_y)$ is a complicated function of k_x and k_y. Instead of showing its explicit form, we plot $\mathcal{K}(k_x, k_y)$ over the Brillouin zone $k_x, k_y \in [0, \pi]$ in Fig. 4 Note that the integrand is peaked at the "hot spot" $Q = (\pi/2, \pi/2)$. This is not surprising because both the Néel and VBS orders have strong nesting at Q.
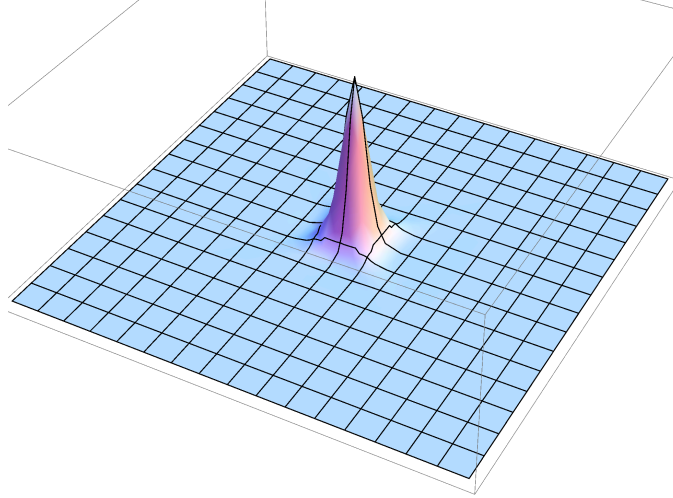
FIG. 4: Plot of $\mathcal{K}$ over a quarter of the Brillouin zone for $t = 1, m = 0.25$.

The other coefficient K' in S_1 can be obtained similarly and is given by:

$$K' = \int dk_0 dk_x dk_y \frac{m^3 t^2 \sin^2 k_x \sin^2 k_y [t^4 (3 \cos^2 k_x + \cos^2 k_y)(\cos^2 k_x + 3 \cos^2 k_y) - 3(k_0^2 + m^2)^2]}{[t^2 (\cos k_x - \cos k_y)^2 + k_0^2 + m^2]^3 [t^2 (\cos k_x + \cos k_y)^2 + k_0^2 + m^2]^3}.$$

Comparing K and K', we found that in general $K \neq K'$. This means that different terms in the effective action (3.4) have different coefficients, so that S cannot be obtained by dimensional reduction from a Chern-Simons term in 6+1 dimensions, which has a single coefficient.

A. Quantum disordered Néel phase

We can now use the results of this section to present an alternative version of the argument in Section II B, that the quantum disordered Néel phase has VBS order. The argument here will be closer in spirit to the duality mapping discussed in Ref. 5.

We will limit our discussion to a quantum-disordered Néel phase where the monopole density is very dilute. Thus, we assume that over a significant intermediate length scale there is an effective description in terms of a theory in which the total Skyrmion number is conserved. As discussed in Section II and Appendix B, we can represent the fluctuations in the local Skyrmion density by a low energy U(1) photon field A_α: by Eq. (2.7), the gauge flux in this field, $\epsilon_{\alpha\beta\gamma}\partial_\beta A_\gamma$, is a quarter the Skyrmion current j_α^N in Eq. (3.6). We can write an effective action of the photons as

$$\mathcal{L}_{\text{eff}} = \frac{1}{2e^2}\left(\epsilon_{\alpha\beta\gamma}\partial_\beta A_\gamma\right)^2 + 4iK j_\alpha^V \epsilon_{\alpha\beta\gamma}\partial_\beta A_\gamma. \tag{3.13}$$

Here the second term represents the topological term in Eq. (3.8). For simplicity, we have

assumed $K' = K$. Different values of K and K' will not affect our conclusion below. Also note that by the discussion at the end of Section II B, $\mathcal{Q}$ is conjugate to j_0^V.

Now let us perform the standard duality transformation of 2+1 dimensional electrodynamics[5,9,28] on $\mathcal{L}_{\text{eff}}$. The first step corresponds to decoupling the Maxwell term by a Hubbard-Stratonovich field, J_α, to obtain

$$\mathcal{L}_{\text{eff}} = \frac{e^2}{8\pi^2} J_\alpha^2 + \frac{i}{2\pi} J_\alpha \epsilon_{\alpha\beta\gamma} \partial_\beta A_\gamma + 4iK j_\alpha^V \epsilon_{\alpha\beta\gamma} \partial_\beta A_\gamma. \tag{3.14}$$

Now, we integrate over A_α, and this yields the constraint

$$J_\alpha = \partial_\alpha \phi - 8\pi K \, j_\alpha^V. \tag{3.15}$$

where ϕ is the scalar field which is dual to the photon. We have judiciously chosen factors of (2π) above to ensure a normalization so that $e^{i\phi}$ is the monopole operator. Finally, inserting Eq. (3.15) into (3.14) we obtain

$$\mathcal{L}_{\text{eff}} = \frac{e^2}{8\pi^2} \left(\partial_\alpha \phi - 8\pi K \, j_\alpha^V \right)^2. \tag{3.16}$$

The effective Lagrangian for the photon phase in Eq. (3.16) allows to conclude that the long-range correlations of $\partial_\alpha \phi$ have the same form as those of j_α^V. In other words, we have the operator correspondence $\partial_\alpha \phi \simeq j_\alpha^V$. In terms of the complex VBS order parameter $V = V_x + iV_y$ we can therefore write for the monopole operator $e^{i\phi} \sim V^\nu$, where ν in general appears to be an irrational number. In the special cases where the value of K was quantized by projection to an integer number of electrons per site[3–5,8,9], ν was found to be an integer; this is a possible value of ν here, although our present methods don't allow us to see why any particular integer would be preferred. The uncertainty in the value of ν here is analogous to the arbitrariness in the overall normalization of $\mathcal{Q}$ in Section II A.

In any case, as long as ν is not an even integer, the correspondence between the monopole operator $e^{i\phi}$ and V^ν implies that V has long-range correlations in the monopole-free region. At even longer scales, once the monpoles condense, the phase of V is locked along one of the lattice directions[8,9].

IV. HONEYCOMB LATTICE

This section will apply the methods developed in Section II and Appendix B to the honeycomb lattice. As is well known, this lattice has an electronic dispersion with a Dirac form at low energies. We will adapt our methods to the Dirac fermions, and find that many results can be computed rapidly in closed form.

The honeycomb lattice has 2 sublattices, and we label the fermions on two sublattices as

c_A and c_B. To begin, we only include Néel order explicitly. Then the analog of Eq. (2.2) is

$$H = -t \sum_{\langle ij \rangle} \left(c_{Ai}^\dagger c_{Bj} + c_{Bj}^\dagger c_{Ai} \right) + m \sum_{i \in A} c_{Ai}^\dagger n^a(\mathbf{r}_i) \sigma^a c_{Ai} - m \sum_{i \in B} c_{Bi}^\dagger n^a(\mathbf{r}_i) \sigma^a c_{Bi}. \qquad (4.1)$$

We restrict to the case with constant Néel order n^a, transform to momentum space, and introduce Pauli matrices τ^a in sublattice space, and obtain

$$\begin{aligned} H = \int \frac{d^2k}{4\pi^2} c^\dagger(\mathbf{k}) \Big[&-t\Big(\cos(\mathbf{k} \cdot \mathbf{e}_1) + \cos(\mathbf{k} \cdot \mathbf{e}_2) + \cos(\mathbf{k} \cdot \mathbf{e}_3) \Big) \tau^x \\ &+ t\Big(\sin(\mathbf{k} \cdot \mathbf{e}_1) + \sin(\mathbf{k} \cdot \mathbf{e}_2) + \sin(\mathbf{k} \cdot \mathbf{e}_3) \Big) \tau^y + m\tau^z n^a \sigma^a \Big] c(\mathbf{k}) \qquad (4.2) \end{aligned}$$

where we have introduced the unit length vectors

$$\mathbf{e}_1 = (1,0) \quad , \quad \mathbf{e}_2 = (-1/2, \sqrt{3}/2) \quad , \quad \mathbf{e}_3 = (-1/2, -\sqrt{3}/2). \qquad (4.3)$$

We also note that we take the origin of co-ordinates of the honeycomb lattice at the center of an empty hexagon, so the A sublattice sites closest to the origin are at $\mathbf{e}_1$, $\mathbf{e}_2$, and $\mathbf{e}_3$, while the B sublattice sites closet to the origin are at $-\mathbf{e}_1$, $-\mathbf{e}_2$, and $-\mathbf{e}_3$.

The low energy electronic excitations reside in the vicinity of the wavevectors $\pm\mathbf{Q}_1$, where $\mathbf{Q}_1 = (4\pi/9)(\mathbf{e}_2 - \mathbf{e}_3)$. So we take the continuum limit in terms of the 8-component field C defined by

$$C_{A1} = c_A(\mathbf{Q}_1) \quad , \quad C_{B1} = c_B(\mathbf{Q}_1) \quad , \quad C_{A2} = c_A(-\mathbf{Q}_1) \quad , \quad C_{B2} = c_B(-\mathbf{Q}_1). \qquad (4.4)$$

In terms of C, we obtain from Eq. (4.2)

$$H = \int \frac{d^2k}{4\pi^2} C^\dagger(\mathbf{k}) \Big(v\tau^y k_x + v\tau^x \rho^z k_y + m\tau^z n^a \sigma^a \Big) C(\mathbf{k}), \qquad (4.5)$$

where $v = 3t/2$; below we set $v = 1$. We have also introduced Pauli matrices ρ^a which act in the $1, 2$ valley space. This is the final form of H: it makes the Dirac structure evident, and will also be the most convenient for our computations.

It is also convenient to list the effects of various symmetry operations on C. Under reflections, $\mathcal{I}_y$, which sends $x \leftrightarrow -x$

$$\mathcal{I}_y: \quad C_{A1} \to C_{B1} \quad , \quad C_{B1} \to C_{A1} \quad , \quad C_{A2} \to C_{B2} \quad , \quad C_{B2} \to C_{A2} \qquad (4.6)$$

Similarly

$$\mathcal{I}_x: \quad C_{A1} \to C_{A2} \quad , \quad C_{B1} \to C_{B2} \quad , \quad C_{A2} \to C_{A1} \quad , \quad C_{B2} \to C_{B1} \qquad (4.7)$$
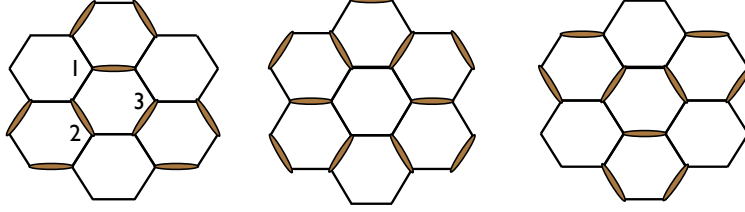
FIG. 5: VBS order on the honeycomb lattice.

Rotations by 60 degrees, R, lead to

$$R: \quad C_{A1} \to \omega^2 C_{B2} \quad , \quad C_{B1} \to \omega C_{A2} \quad , \quad C_{A2} \to \omega C_{B1} \quad , \quad C_{B2} \to \omega^2 C_{A1} \tag{4.8}$$

Translation by the unit cell vector $\mathbf{e}_2 - \mathbf{e}_3$, T_y:

$$T_y: \quad C_{A1} \to \omega^2 C_{A1} \quad , \quad C_{B1} \to \omega^2 C_{B1} \quad , \quad C_{A2} \to \omega C_{A2} \quad , \quad C_{B2} \to \omega C_{B2} \tag{4.9}$$

Time reversal $t \to -t$:

$$\mathcal{T}: \quad C_{A1} \to i\sigma^y C_{A2} \quad , \quad C_{A2} \to i\sigma^y C_{A1} \quad , \quad C_{B1} \to i\sigma^y C_{B2}, \quad C_{B2} \to i\sigma^y C_{B1} \tag{4.10}$$

Notice that time reversal transformation also involves a complex conjugation transformation.

From these transformations, we can construct the fermion bilinear associated with the kekule VBS pattern shown in Fig 5. In terms of the continuum field C, the VBS order parameter is

$$V = C^\dagger \tau^x (\rho^x + i\rho^y) C \tag{4.11}$$

We can verify this is the VBS order with the kekule pattern of Fig. 5 by its symmetry transformations

$$\begin{aligned} \mathcal{I}_y &: V \to V \\ \mathcal{I}_x &: V \to V^* \\ R &: V \to V^* \\ T_y &: V \to \omega^2 V \\ \mathcal{T} &: V \to V^*. \end{aligned} \tag{4.12}$$

A. 6D method

In the present situation with a Dirac fermion spectrum, the dimensional reduction method[23,24] from 6D does apply, and be used to compute the coupling between the fluctuating Néel and VBS orders. From Eqs. (4.5) and (4.11), we can write down the explicit

form of the Hamiltonian in the 8×8 space of Dirac fermions:

$$H(\mathbf{k}, k_1, k_2, k_3, k_4) =$$
$$\tau^y k_x + \tau^x \rho^z k_y + \tau^x \rho^x k_1 + \tau^x \rho^y k_2 + \tau^z \sigma^x k_3 + \tau^z \sigma^y k_4 + m\tau^z \sigma^z n^z. \qquad (4.13)$$

Here $\mathbf{k} = (k_x, k_y)$, and the 'extra-dimensional' momenta $k_{1,2,3,4}$ are related to the order parameters: $k_1 = V_x$, $k_2 = V_y$, $k_3 = n^x$, and $k_4 = n^y$. Now note that the matrices in all the terms in Eq. (4.13) anti-commute with each other. So this has the natural interpretation as 6D Dirac Hamiltonian, where the last term proportional to m has the interpretation of a Dirac fermion mass. We can now proceed as in Ref. 19, and derive the WZW term for the order parameters.

B. U(1) gauge theory

Next we turn to the analog of the analysis in Section II A for the square lattice. However, rather than working with the spatially varying Néel order as in Eq. (2.2), we will use the U(1) gauge field formulation of Eq. (2.5) which was applied to the square lattice in Appendix B.

We begin with the ψ fermion Hamiltonian in Eq. (2.5) and take its continuum limit as in Eq. (4.5). For this, we make the analog of the transformation in Eq. (4.4) from the lattice ψ fermions to continuum Ψ fermions. In this manner, we obtain the continuum U(1) gauge theory

$$\mathcal{L} = \Psi^\dagger \left(\partial_\tau - i\sigma^z A_\tau - i\tau^y (\partial_x - i\sigma^z A_x) - i\tau^x \rho^z (\partial_y - i\sigma^z A_y) + m\tau^z \sigma^z \right) \Psi \qquad (4.14)$$

Now we obtain the result which is the analog of Eq. (B10) by applying the Kubo formula to determine the response in an arbitrary fermion bilinear $\Psi^\dagger \Gamma \Psi$ due to an arbitrary slowly varying A_α. This involves evaluating a diagram with one fermion loop, and the long wavelength result is

$$\langle \Psi^\dagger \Gamma \Psi \rangle = \frac{1}{8\pi} \Big\{ (\partial_x A_\tau - \partial_\tau A_x) \mathrm{Tr}\left[\Gamma \tau^x \right] + (\partial_\tau A_y - \partial_y A_\tau) \mathrm{Tr}\left[\Gamma \rho^z \tau^y \right]$$
$$+ (\partial_y A_x - \partial_x A_y) \mathrm{Tr}\left[\Gamma \rho^z \right] \Big\}. \qquad (4.15)$$

Now we see that the choices $\Gamma = \tau^x$, $\rho^z \tau^y$, and ρ^z lead to non-zero fermion bilinears induced by the A_α gauge flux. Note that this result was obtained with much greater ease in the continuum Dirac theory than for Eq. (B10).

Let us restate the result in Eq. (4.15) in different terms. We add to $\mathcal{L}$ in Eq. (4.14) a source term j_α^V:

$$\mathcal{L} \to \mathcal{L} - \frac{i}{2} \left(j_0^V \Psi^\dagger \rho^z \Psi + j_x^V \Psi^\dagger \rho^z \tau^y \Psi + j_y^V \Psi^\dagger \tau^x \Psi \right). \qquad (4.16)$$

20

Then the implication of Eq. (4.16) is that if we integrate out the Ψ fermions, the effective action for j_α^V and the gauge field A_α has a mutual Chern-Simons term:

$$\mathcal{L}_{\text{eff}} = \frac{1}{12\pi m}(\epsilon_{\alpha\beta\gamma}\partial_\beta A_\gamma)^2 + \frac{i}{2\pi}j_\alpha^V \epsilon_{\alpha\beta\gamma}\partial_\beta A_\gamma \tag{4.17}$$

The similarity to Eq. (3.14) should now be evident. We can now proceed with the duality of electrodynamics to obtain the analog of Eq. (3.16), which is

$$\mathcal{L}_{\text{eff}} = \frac{3m}{8\pi}\left(\partial_\alpha\phi - j_\alpha^V\right)^2, \tag{4.18}$$

where again $e^{i\phi}$ is the monopole operator. As argued below Eq. (3.16) any operator with the same quantum numbers as $e^{i\phi}$ has long-range order in the 'quantum-disordered' phase.

Here we present a different route to identifying candidates for the competing order. First, we notice that the theory in Eq. (4.16) actually enjoys a gauge invariance under which

$$\Psi \to \exp\left(i\frac{\rho^z}{2}\theta\right)\Psi \quad , \quad j_\alpha^V \to j_\alpha^v - \partial_\alpha\theta \tag{4.19}$$

where θ is a field with an arbitrary spacetime dependence. (Note that this gauge invariance is completely different from that associated with the A_α gauge field, under which $\Psi \to \exp((i/2)\sigma^z\theta')\Psi$.) Now we observe that this gauge invariance extends also to Eq. (4.19), under which

$$e^{i\phi} \to e^{i\theta}e^{i\phi}. \tag{4.20}$$

We will use Eq. (4.20) as the key relation needed for any competing order associated with the monopole operator $e^{i\phi}$.

Equivalently, we can use Eq. (4.19), and restate the requirement of Eq. (4.20) as the commutation relation

$$[\mathcal{Q}, e^{i\phi(\mathbf{x})}] = e^{i\phi(\mathbf{x})}, \tag{4.21}$$

where

$$\mathcal{Q} = \frac{1}{2}\int d^2r\, \Psi^\dagger \rho^z \Psi. \tag{4.22}$$

This makes a very explicit connection to Section II B and Eq. (2.28). Note that here the overall normalization of $\mathcal{Q}$ is specified, and does not suffer from the arbitrariness we encountered in Sections II A and III A.

Now we can easily check that the VBS order parameter in Eq. (4.11) obeys the commutation relation

$$[\mathcal{Q}, V(\mathbf{x})] = V(\mathbf{x}), \tag{4.23}$$

21

and so we conclude that $e^{i\phi} \simeq V$, and that VBS order can appear in the quantum-disordered Néel phase.

C.   Other competing orders

In addition to the VBS order parameter V, it is now easy to see that there are other order parameters which are canonically conjugate to $\mathcal{Q}$. For instance, the following three complex order parameters all satisfy Eq. 4.23:

$$V_1 \sim \Psi^\dagger(\rho^x + i\rho^y)\Psi, \; V_2 \sim \Psi^\dagger\tau^z(\rho^x + i\rho^y)\Psi, \; V_3 \sim \Psi^\dagger\tau^y(\rho^x + i\rho^y)\Psi. \tag{4.24}$$

Under discrete symmetries, these order parameters transform as

$$\mathcal{I}_y : V_1 \to V_1 \quad , \quad V_2 \to -V_2 \quad , \quad V_3 \to -V_3, \tag{4.25}$$

$$\mathcal{I}_x : V_\mu \to V_\mu^* \tag{4.26}$$

$$R : \mathrm{Re}[V_1] + i\mathrm{Im}[V_2] \to \omega^2(\mathrm{Re}[V_1] + i\mathrm{Im}[V_2]), \tag{4.27}$$

$$\mathrm{Re}[V_2] + i\mathrm{Im}[V_1] \to -\omega^2(\mathrm{Re}[V_2] + i\mathrm{Im}[V_1]), \tag{4.28}$$

$$V_3 \to -V_3^* \tag{4.29}$$

$$T_y : V_\mu \to \omega^2 V_\mu \tag{4.30}$$

$$T : V_1 \to V_1^* \quad , \quad V_2 \to V_2^* \quad , \quad V_3 \to -V_3^*. \tag{4.31}$$

According to these transformation laws, we can identify that V_1 is a charge density wave (CDW) with wave vector $2\mathbf{Q}_1$, V_2 is the $A-B$ sublattice staggered CDW, and V_3 is a charge current density wave.

However, notice that the matrices in V in Eq. (4.11) anticommute with all the matrices in H in Eq. (4.5); therefore the VBS state has the lowest fermionic mean field energy, because the fermion Ψ will acquire a Dirac mass gap $m \sim \sqrt{m^2 + |V|^2}$. Compared with the VBS order parameter V, the other three order parameters V_μ have higher mean field fermion energy, hence are less favorable in energy.

D.   Superconductor order parameters

In addition to the VBS order parameter, the Néel order can also have strong competition with superconductor, as long as the SC order parameters satisfy Eq. 4.21. In this section we will focus on spin singlet pairings. Using the quantum number $\mathcal{Q}$ in Eq. 4.22 and criterion Eq. 4.21, it is straightforward to show that the following six groups of SC order parameters are candidate competing orders of the Néel order:

$$\text{Group 1}: \quad (\Delta_1, \; \Delta_2) \sim (\mathrm{Re}[\Psi^t i\sigma^y\Psi], \; \mathrm{Im}[\Psi^t i\sigma^y\rho^z\Psi]),$$

$$\Delta_1 \sim \sum_k C_{A,\mathbf{Q}_1+k} i\sigma^y C_{A,\mathbf{Q}_1-k} + C_{B,\mathbf{Q}_1+k} i\sigma^y C_{B,\mathbf{Q}_1-k}$$

$$+ C_{A,-\mathbf{Q}_1+k} i\sigma^y C_{A,-\mathbf{Q}_1-k} + C_{B,-\mathbf{Q}_1+k} i\sigma^y C_{B,-\mathbf{Q}_1-k} + H.c.$$

$$\Delta_2 \sim \sum_k i C_{A,\mathbf{Q}_1+k} i\sigma^y C_{A,\mathbf{Q}_1-k} + i C_{B,\mathbf{Q}_1+k} i\sigma^y C_{B,\mathbf{Q}_1-k}$$

$$- i C_{A,-\mathbf{Q}_1+k} i\sigma^y C_{A,-\mathbf{Q}_1-k} - i C_{B,-\mathbf{Q}_1+k} i\sigma^y C_{B,-\mathbf{Q}_1-k} + H.c.$$

Group 2 : $(\Delta_1, \ \Delta_2) \sim (\mathrm{Im}[\Psi^t i\sigma^y \Psi], \ \mathrm{Re}[\Psi^t i\sigma^y \rho^z \Psi]),$

$$\Delta_1 \sim \sum_k i C_{A,\mathbf{Q}_1+k} i\sigma^y C_{A,\mathbf{Q}_1-k} + i C_{B,\mathbf{Q}_1+k} i\sigma^y C_{B,\mathbf{Q}_1-k}$$

$$+ i C_{A,-\mathbf{Q}_1+k} i\sigma^y C_{A,-\mathbf{Q}_1-k} + i C_{B,-\mathbf{Q}_1+k} i\sigma^y C_{B,-\mathbf{Q}_1-k} + H.c.$$

$$\Delta_2 \sim \sum_k C_{A,\mathbf{Q}_1+k} i\sigma^y C_{A,\mathbf{Q}_1-k} + C_{B,\mathbf{Q}_1+k} i\sigma^y C_{B,\mathbf{Q}_1-k}$$

$$- C_{A,-\mathbf{Q}_1+k} i\sigma^y C_{A,-\mathbf{Q}_1-k} - C_{B,-\mathbf{Q}_1+k} i\sigma^y C_{B,-\mathbf{Q}_1-k} + H.c.$$

Group 3 : $(\Delta_1, \ \Delta_2) \sim (\mathrm{Re}[\Psi^t \tau^z i\sigma^y \Psi], \ \mathrm{Im}[\Psi^t \tau^z i\sigma^y \rho^z \Psi])$

$$\Delta_1 \sim \sum_k C_{A,\mathbf{Q}_1+k} i\sigma^y C_{A,\mathbf{Q}_1-k} - C_{B,\mathbf{Q}_1+k} i\sigma^y C_{B,\mathbf{Q}_1-k}$$

$$+ C_{A,-\mathbf{Q}_1+k} i\sigma^y C_{A,-\mathbf{Q}_1-k} - C_{B,-\mathbf{Q}_1+k} i\sigma^y C_{B,-\mathbf{Q}_1-k} + H.c.$$

$$\Delta_2 \sim \sum_k i C_{A,\mathbf{Q}_1+k} i\sigma^y C_{A,\mathbf{Q}_1-k} - i C_{B,\mathbf{Q}_1+k} i\sigma^y C_{B,\mathbf{Q}_1-k}$$

$$- i C_{A,-\mathbf{Q}_1+k} i\sigma^y C_{A,-\mathbf{Q}_1-k} + i C_{B,-\mathbf{Q}_1+k} i\sigma^y C_{B,-\mathbf{Q}_1-k} + H.c.$$

Group 4 : $(\Delta_1, \ \Delta_2) \sim (\mathrm{Im}[\Psi^t \tau^z i\sigma^y \Psi], \ \mathrm{Re}[\Psi^t \tau^z i\sigma^y \rho^z \Psi])$

$$\Delta_1 \sim \sum_k i C_{A,\mathbf{Q}_1+k} i\sigma^y C_{A,\mathbf{Q}_1-k} - i C_{B,\mathbf{Q}_1+k} i\sigma^y C_{B,\mathbf{Q}_1-k}$$

$$+ i C_{A,-\mathbf{Q}_1+k} i\sigma^y C_{A,-\mathbf{Q}_1-k} - i C_{B,-\mathbf{Q}_1+k} i\sigma^y C_{B,-\mathbf{Q}_1-k} + H.c.$$

$$\Delta_2 \sim \sum_k C_{A,\mathbf{Q}_1+k} i\sigma^y C_{A,\mathbf{Q}_1-k} - C_{B,\mathbf{Q}_1+k} i\sigma^y C_{B,\mathbf{Q}_1-k}$$

$$-C_{A,-\mathbf{Q}_1+k}i\sigma^y C_{A,-\mathbf{Q}_1-k} + C_{B,-\mathbf{Q}_1+k}i\sigma^y C_{B,-\mathbf{Q}_1-k} + H.c.$$

Group 5 : $(\Delta_1,\ \Delta_2) \sim (\mathrm{Re}[\Psi^t \tau^x i\sigma^y \Psi],\ \mathrm{Im}[\Psi^t \tau^x i\sigma^y \rho^z \Psi])$

$$\Delta_1 \sim \sum_k C_{A,\mathbf{Q}_1+k}i\sigma^y C_{B,\mathbf{Q}_1-k} + C_{B,\mathbf{Q}_1+k}i\sigma^y C_{A,\mathbf{Q}_1-k}$$

$$+C_{A,-\mathbf{Q}_1+k}i\sigma^y C_{B,-\mathbf{Q}_1-k} + C_{B,-\mathbf{Q}_1+k}i\sigma^y C_{A,-\mathbf{Q}_1-k} + H.c.$$

$$\Delta_2 \sim \sum_k iC_{A,\mathbf{Q}_1+k}i\sigma^y C_{B,\mathbf{Q}_1-k} + iC_{B,\mathbf{Q}_1+k}i\sigma^y C_{A,\mathbf{Q}_1-k}$$

$$-iC_{A,-\mathbf{Q}_1+k}i\sigma^y C_{B,-\mathbf{Q}_1-k} - iC_{B,-\mathbf{Q}_1+k}i\sigma^y C_{A,-\mathbf{Q}_1-k} + H.c.$$

Group 6 : $(\Delta_1,\ \Delta_2) \sim (\mathrm{Im}[\Psi^t \tau^x i\sigma^y \Psi],\ \mathrm{Re}[\Psi^t \tau^x i\sigma^y \rho^z \Psi])$

$$\Delta_1 \sim \sum_k iC_{A,\mathbf{Q}_1+k}i\sigma^y C_{B,\mathbf{Q}_1-k} + iC_{B,\mathbf{Q}_1+k}i\sigma^y C_{A,\mathbf{Q}_1-k}$$

$$+iC_{A,-\mathbf{Q}_1+k}i\sigma^y C_{B,-\mathbf{Q}_1-k} + iC_{B,-\mathbf{Q}_1+k}i\sigma^y C_{A,-\mathbf{Q}_1-k} + H.c.$$

$$\Delta_2 \sim \sum_k C_{A,\mathbf{Q}_1+k}i\sigma^y C_{B,\mathbf{Q}_1-k} + C_{B,\mathbf{Q}_1+k}i\sigma^y C_{A,\mathbf{Q}_1-k}$$

$$-C_{A,-\mathbf{Q}_1+k}i\sigma^y C_{B,-\mathbf{Q}_1-k} - C_{B,-\mathbf{Q}_1+k}i\sigma^y C_{A,-\mathbf{Q}_1-k} + H.c. \tag{4.32}$$

All of these SC order parameters carry nonzero lattice momentum $2\mathbf{Q}_1$, and none of them gaps out the Dirac points. Nevertheless, these SC orders are most likely to be adjacent to the Néel order on the phase diagram.

V.   NAMBU QUASI-PARTICLES OF $d-$WAVE SUPERCONDUCTOR

In this section we will apply the above methods to analyze the $d-$wave superconductor and its descendants. As in previous section we will examine the nature of the "quantum disordered" phase after loss of antiferromagnetic order. However, we will not consider the case of commensurate antiferromagnetic ordering at wavevector $\mathbf{Q} = (\pi, \pi)$, because it requires computations we have not explored here. Rather, we will limit ourselves to the technically easier case of nested spin density wave order, with a wavevector precisely equal to the separation between two of the nodal points of the fermionic excitations of the d-wave superconductor. The non-nested case is of experimental importance, but we will not consider it here.

The nodal quasi-particles of the d-wave superconductor are described by the following Dirac fermion Lagrangian:

$$L_\Psi = \Psi_1^\dagger(\partial_\tau - i\frac{v_F}{\sqrt{2}}(\partial_x + \partial_y)\tau^z - i\frac{v_\Delta}{\sqrt{2}}(-\partial_x + \partial_y)\tau^x)\Psi_1$$

$$+ \Psi_2^\dagger(\partial_\tau - i\frac{v_F}{\sqrt{2}}(-\partial_x + \partial_y)\tau^z - i\frac{v_\Delta}{\sqrt{2}}(\partial_x + \partial_y)\tau^x)\Psi_2. \quad (5.1)$$

$\Psi_1 = (f_1, i\sigma^y f_3^\dagger)^t$, $\Psi_2 = (f_2, i\sigma^y f_4^\dagger)^t$. f_1, f_2, f_3 and f_4 are quasiparticles at nodal points (Q,Q), $(-Q,Q)$, $(-Q,-Q)$ and $(Q,-Q)$ respectively. Notice that Q is in general incommensurate, v_F and v_Δ are different from each other.

We assume the system has the symmetry of the square lattice. Under square lattice discrete symmetry group, the quasi-particle Ψ_1 and Ψ_2 transform as:

$$T_x, \quad x \to x+1, \quad \Psi_1 \to e^{iQ}\Psi_1, \quad \Psi_2 \to e^{-iQ}\Psi_2;$$

$$T_y, \quad y \to y+1, \quad \Psi_1 \to e^{iQ}\Psi_1, \quad \Psi_2 \to e^{iQ}\Psi_2;$$

$$\mathcal{I}_y, \quad x \to -x, \quad \Psi_1 \to \Psi_2, \quad \Psi_2 \to \Psi_1;$$

$$\mathcal{I}_x, \quad y \to -y, \quad \Psi_1 \to \sigma^y\tau^y\Psi_2^\dagger, \quad \Psi_2 \to \sigma^y\tau^y\Psi_1^\dagger;$$

$$\mathcal{I}_{x-y}, \quad x \to y, \quad y \to x, \quad \Psi_1 \to i\tau^z\Psi_1, \quad \Psi_2 \to \sigma^y\tau^x\Psi_2^\dagger;$$

$$\mathcal{I}_{x+y}, \quad x \to -y, \quad y \to -x, \quad \Psi_1 \to \sigma^y\tau^x\Psi_1^\dagger, \quad \Psi_2 \to i\tau^z\Psi_2;$$

$$T, \quad t \to -t, \quad \Psi_1 \to i\tau^y\Psi_1^\dagger, \quad \Psi_2 \to i\tau^y\Psi_2^\dagger. \quad (5.2)$$

Notice that transformations $\mathcal{I}_{x-y}$ and $\mathcal{I}_{x+y}$ are combined with a U(1) transformation on the superconductor order parameter: $\Delta e^{i\theta} \to \Delta e^{i\theta+i\pi}$.

Now let us consider the spin density wave states that gap out the nodal quasi-particles *i.e.* the SDW with wave vector $(2Q, 2Q)$, and $(2Q, -2Q)$, which can be written as $i\Psi_1^t\tau^y\sigma^y\vec{\sigma}\Psi_1$ and $i\Psi_2^t\tau^y\sigma^y\vec{\sigma}\Psi_2$ respectively. In contrast, the SDW at $(2Q, 0)$ and $(0, 2Q)$ will not gap out the nodes, and they will be ignored hereafter. It is convenient to introduce the Majorana fermion χ_a as $\Psi = \chi_A + i\chi_B$, and there are in total four different choices of SDW that can gap out the nodal points:

$$\vec{\Phi}_1 = \text{Re}[i\Psi^t\tau^y\sigma^y\vec{\sigma}\Psi] \sim (\chi^t i\tau^y\sigma^y\sigma^x\rho^z\chi, \ \chi^t\tau^y\sigma^y\sigma^y\rho^x\chi, \ \chi^t i\tau^y\sigma^y\sigma^z\rho^z\chi),$$

$$\vec{\Phi}_2 = \text{Re}[i\Psi^t\tau^y\sigma^y\vec{\sigma}\mu^z\Psi] \sim (\chi^t i\tau^y\sigma^y\sigma^x\rho^z\mu^z\chi, \ \chi^t\tau^y\sigma^y\sigma^y\rho^x\mu^z\chi, \ \chi^t i\tau^y\sigma^y\sigma^z\rho^z\mu^z\chi),$$

$$\vec{\Phi}_3 = \text{Im}[i\Psi^t\tau^y\sigma^y\vec{\sigma}\Psi] \sim (\chi^t i\tau^y\sigma^y\sigma^x\rho^x\chi, \ \chi^t\tau^y\sigma^y\sigma^y\rho^z\chi, \ \chi^t i\tau^y\sigma^y\sigma^z\rho^x\chi),$$

$$\vec{\Phi}_4 = \text{Im}[i\Psi^t\tau^y\sigma^y\vec{\sigma}\mu^z\Psi] \sim (\chi^t i\tau^y\sigma^y\sigma^x\rho^x\mu^z\chi, \ \chi^t\tau^y\sigma^y\sigma^y\rho^z\mu^z\chi, \ \chi^t i\tau^y\sigma^y\sigma^z\rho^x\mu^z\chi). \quad (5.3)$$

The Pauli matrices μ^a mix Ψ_1 and Ψ_2, while the Pauli matrices ρ^a mix χ_A and χ_B. In the Majorana Fermion basis, the SU(2) spin operators are represented by the total antisymmetric matrices

$$\vec{S} = (\sigma^x\rho^y, \ \sigma^y, \ \sigma^z\rho^y). \quad (5.4)$$

We can check that all four vectors $\vec{\Phi}_a$ ($a = 1 \cdots 4$) transform as vectors under $\vec{S}$.

Mow we hope to consider the slowly varying SDW by introducing the SU(2) gauge field $\sum_l A^l_\mu S^l$, which will be Higgsed to U(1) gauge field with a background nonzero expectation value of Φ_a:

$$
\begin{aligned}
L_\chi &= \chi^t_1((\partial_\tau - iA^l_0 S^l) - iv_F(\partial_X - iA^l_X S^l)\tau^z - iv_\Delta(\partial_Y - iA^l_Y S^l)\tau^x)\chi_1 \\
&+ \chi^\dagger_2((\partial_\tau - iA^l_0 S^l) - iv_F(\partial_Y - iA^l_Y S^l)\tau^z - iv_\Delta(\partial_X - iA^l_X S^l)\tau^x)\chi_2 \\
&+ \Phi^l_a\chi^t T^l_a\chi. \quad (5.5)
\end{aligned}
$$

Now we have redefined the coordinate $(x+y)/\sqrt{2} \to X$, $(-x+y)/\sqrt{2} \to Y$. The order parameter Φ^l_a has Higgsed the SU(2) gauge field down to U(1) gauge field A^l_μ. The matrix T^l_a can be found in Eq. 5.3.

Now the flux quantum number can be calculated using the same techniques developed in the previous sections. We summarize our results in the following:

$$\text{Group 1} : \langle\Phi^l_1\rangle \neq 0, \quad \text{gauge flux carries } \mathcal{Q} \sim \chi^t\sigma^y\mu^z\rho^x\chi;$$

$$\text{Group 2} : \langle\Phi^l_2\rangle \neq 0, \quad \text{gauge flux carries } \mathcal{Q} \sim \chi^t\sigma^y\rho^x\chi,$$

$$\text{Group 3} : \langle\Phi^l_3\rangle \neq 0, \quad \text{gauge flux carries } \mathcal{Q} \sim \chi^t\sigma^y\mu^z\rho^z\chi,$$

$$\text{Group 4} : \langle\Phi^l_4\rangle \neq 0, \quad \text{gauge flux carries } \mathcal{Q} \sim \chi^t\sigma^y\rho^z\chi. \quad (5.6)$$

The quantum number $\mathcal{Q}$ carried by the flux is obviously SU(2) gauge invariant.

The flux condensate will again lead to orders that break certain lattice symmetry in Eq. 5.2. The condensate order parameter V has to satisfy Eq. 2.28. Within all these order parameters that satisfy Eq. 2.28, we choose the order parameters that have the lowest nodal quasi-particle mean field energy, *i.e.* the order parameters that anticommute with T^l_a. We

list our results in the following equation, and for each group of SDW in Eq. 5.3 we introduce a five component vector $\Xi^i_{(a)}$ with $\vec{\Phi}_a \sim (\Xi^1_{(a)}, \Xi^2_{(a)}, \Xi^3_{(a)})$, $V_a \sim \Xi^4_{(a)} + i\Xi^5_{(a)}$:

$$\text{Group 1} : \Xi^{i=1,2,3}_{(1)} = \vec{\Phi}_1,$$

$$\Xi^4_{(1)} = \frac{1}{\sqrt{2}}\chi^t(\tau^z - \tau^x)\mu^y\chi \sim \Psi^\dagger(\tau^z - \tau^x)\mu^y\Psi,$$

$$\Xi^5_{(1)} = \chi^t(\tau^z - \tau^x)\mu^x\sigma^y\rho^x\chi \sim \text{Im}[\Psi^t(\tau^z - \tau^x)\mu^x\sigma^y\Psi];$$

$$\text{Group 2} : \Xi^{i=1,2,3}_{(2)} = \vec{\Phi}_2,$$

$$\Xi^4_{(2)} = \frac{1}{\sqrt{2}}\chi^t(\tau^z - \tau^x)\rho^y\mu^x\chi \sim \Psi^\dagger(\tau^z - \tau^x)\mu^x\Psi,$$

$$\Xi^5_{(2)} = \frac{1}{\sqrt{2}}\chi^t(\tau^z - \tau^x)\mu^x\sigma^y\rho^z\chi \sim \text{Re}[\Psi^t(\tau^z - \tau^x)\sigma^y\mu^x\Psi];$$

$$\text{Group 3} : \Xi^{i=1,2,3}_{(3)} = \vec{\Phi}_3,$$

$$\Xi^4_{(3)} = \Xi^4_{(1)} = \frac{1}{\sqrt{2}}\chi^t(\tau^z - \tau^x)\mu^y\chi \sim \Psi^\dagger(\tau^z - \tau^x)\mu^y\Psi,$$

$$\Xi^5_{(3)} = \Xi^5_{(2)} \frac{1}{\sqrt{2}}\chi^t(\tau^z - \tau^x)\mu^x\sigma^y\rho^z\chi \sim \text{Re}[\Psi^t(\tau^z - \tau^x)\mu^x\sigma^y\Psi];$$

$$\text{Group 4} : \Xi^{i=1,2,3}_{(4)} = \vec{\Phi}_4,$$

$$\Xi^4_{(4)} = \Xi^4_{(2)} = \frac{1}{\sqrt{2}}\chi^t(\tau^z - \tau^x)\rho^y\mu^x\chi \sim \Psi^\dagger(\tau^z - \tau^x)\mu^x\Psi.$$

$$\Xi^5_{(4)} = \Xi^5_{(1)} = \frac{1}{\sqrt{2}}\chi^t(\tau^z - \tau^x)\mu^x\sigma^y\rho^x\chi \sim \text{Im}[\Psi^t(\tau^z - \tau^x)\mu^x\sigma^y\Psi]. \quad (5.7)$$

With the formalism developed in Ref.[19], we can also show that there is a O(5) WZW term for each group of O(5) vector $\Xi^i_{(a)}$. Both the WZW term and the gauge flux calculations imply that the SDW $\Phi^i_{(a)}$ and order parameters $V_a \sim \Xi^4_{(a)} + i\Xi^5_{(a)}$ are competing with each other, and after suppressing the SDW $\Phi^i_{(a)}$, the system enters the order with nonzero $\langle V_a \rangle$ directly.

Now we want to identify the physical meanings of $\Xi^4_{(a)}$ and $\Xi^5_{(a)}$. Clearly, $\Xi^4_{(a)}$ and $\Xi^5_{(b)}$ are both density waves of physical quantities, with wave vectors $(2Q, 0)$ and $(0, 2Q)$ respectively. Under lattice symmetry Eq. 5.2, $\Xi^4_{(a)}$ and $\Xi^5_{(a)}$ transforms as:

$$\mathcal{I}_y : \Xi^4_{(1)} \to -\Xi^4_{(1)}, \quad \Xi^5_{(1)} \to \Xi^5_{(1)}, \quad \Xi^4_{(2)} \to \Xi^4_{(2)}, \quad \Xi^5_{(2)} \to \Xi^5_{(2)},$$

$$\mathcal{I}_x \; : \; \Xi^4_{(1)} \to \Xi^4_{(1)}, \quad \Xi^5_{(1)} \to \Xi^5_{(1)}, \quad \Xi^4_{(2)} \to \Xi^4_{(2)}, \quad \Xi^5_{(2)} \to -\Xi^5_{(2)},$$

$$\mathcal{I}_{x-y} \; : \; \Xi^4_{(1)} \leftrightarrow \Xi^5_{(2)}, \quad \Xi^5_{(1)} \leftrightarrow \Xi^4_{(2)},$$

$$\mathcal{I}_{x+y} \; : \; \Xi^4_{(1)} \leftrightarrow \Xi^5_{(2)}, \quad \Xi^5_{(1)} \leftrightarrow \Xi^4_{(2)},$$

$$T \; : \; \Xi^i_{(a)} \to \Xi^i_{(a)}, \quad i = 4, \; 5. \tag{5.8}$$

According to these transformations, we can make the following identifications:

$$\Xi^4_{(2)} + i\Xi^4_{(1)} = \Xi^4_{(4)} + i\Xi^4_{(3)} = \text{VBS or CDW with wave vector } (2Q, \; 0);$$

$$\Xi^5_{(1)} + i\Xi^5_{(2)} = \Xi^5_{(4)} + i\Xi^5_{(3)} = \text{VBS or CDW with wave vector } (0, \; 2Q). \tag{5.9}$$

These analysis suggests that the SDW at wave vectors $(2Q, 2Q)$ and $(2Q, -2Q)$ is competing with CDW/VBS order parameters at $(2Q, 0)$ and $(0, 2Q)$, and the suppression of the SDW leads to the emerging of CDW/VBS order parameters.

VI. CONCLUSIONS

This paper has addressed a problem of long-standing interest in the study of correlated electron systems in two spatial dimensions. Many such systems have insulating, metallic, or superconducting ground states with long-range antiferromagnetic order. By tuning the electron concentration, pressure, or the values of exchange constants in model systems, it is possible to drive a quantum phase transition to a phase where the antiferromagnetic order is lost. We are interested in the nature of the "quantum-disordered" phase so obtained.

For certain insulating square or honeycomb lattice models, the essential features were understood some time ago[3,4]: the lattice spins endow point spacetime defects in the Néel order ('hedgehogs') with geometric (or Berry) phases, which lead to valence bond solid (VBS) order in the quantum-disordered phase. Here we have presented a more general version of this argument, in principle applicable to arbitrary insulating, metallic, or superconducting electronic systems in two dimensions, with general band structures. The key step was to associate the geometric phases with bands of one electron states in the background of local antiferromagnetic order. The antiferromagnetic order was then allowed to have a spacetime variation in orientation (but *not* in magnitude) so that there was no long-range antiferromagnetic order, thus accessing the quantum-disordered phase. We found that the skyrmion density in this local antiferromagnetic order induced a response in an electronic bilinear conjugate to the competing order: this is contained in our key result in Eq. (2.22).

Our main application of these results was to cases in which the electronic band structure

was fully gapped in the phase with antiferromagnetic order: we considered square lattice insulators in Section II, honeycomb lattice insulators in Section IV, and d-wave superconductors with spin density wave order nesting the nodal points in Section V. We obtained VBS order in many cases, but also found a number of other possible orderings.

However, in principle, the result Eq. (2.22) applies also in cases where the antiferromagnetic order does not fully gap the electron bands $e.g.$ when there are hole and/or electron pockets. Such a situation is clearly of importance for the underdoped cuprate superconductors. The result in Eq. (2.22) contains a singular dependence on $\mathbf{k}$ at the Fermi surfaces of such band structures, and this is likely of importance in the quantum-disordered phase. Alternatively, expressions for the coupling K in Section III would acquire long-ranged corrections due to Fermi surface singularities. We leave the elucidation of such effects to future work. However, if we ignore such effects, the arguments of Section III A would apply also to this metallic case, with a variable exponent ν relating the monopole operator to the VBS order. The net result is that any ordering associated with an integer power of V is possible. Interestingly the same conclusion was reached in an earlier study[29] of quantum disordered Néel states in a compressible background using a toy model of bosons.

Appendix A: Rotor theory of Hubbard model

This appendix will show how the decomposition in Eq. (2.3) can be used to write an exact path integral representation of an arbitrary Hubbard-like model. The z_α becomes co-ordinates of an O(4) rotor in this path integral, and so do not directly contribute to the geometric phases of interest in this paper. This is to be contrasted from the alternative Schwinger boson formulation, where the canonical nature of the Schwinger bosons ensures that they carry the entire geometric phase at half-filling[5].

We consider a Hubbard model on a general lattice

$$H = H_0 + H_1 \tag{A1}$$

where H_0 has the single site terms

$$H_0 = \sum_i \left[U \left(n_{i\uparrow} - \frac{1}{2} \right) \left(n_{i\downarrow} - \frac{1}{2} \right) - \mu(n_{i\uparrow} + n_{i\downarrow}) \right] \tag{A2}$$

and H_1 is the hopping term

$$H_1 = -\sum_{i<j} t_{ij} c_{i\alpha}^\dagger c_{j\alpha} \tag{A3}$$

As in Eq. (2.3), we transform the electron to a rotating reference frame expressed in terms of the spinless fermions c_p and the complex unit spinor z_α. Here, it is useful to write z_α in real and imaginary parts:

$$z_\uparrow = \phi_0 + i\phi_1 \quad , \quad z_\downarrow = \phi_2 + i\phi_3. \tag{A4}$$

The inner product of two complex spinors is

$$\tilde{z}_\alpha^* z_\alpha = \tilde{\phi}(1 - \rho^y)\phi \tag{A5}$$

We will use σ^a for Pauli matrices in the $\uparrow, \downarrow$ space, and ρ^a for Pauli matrices in the real/imaginary space. The global spin rotation

$$z \to \left(1 + i\theta^a \sigma^a\right) z \tag{A6}$$

acts on ϕ via

$$\phi \to \left(1 + i\theta^a S^a\right)\phi, \tag{A7}$$

where S^a are the antisymmetric Hermitian matrices

$$S^x = -\sigma^x \rho^y \quad , \quad S^y = \sigma^y \quad , \quad S^z = -\sigma^z \rho^y. \tag{A8}$$

Combining (A5) and (A6) we have

$$z^* \sigma^a z = \phi(1 - \rho^y) S^a \phi = -\phi \rho^y S^a \phi. \tag{A9}$$

The SU(2) gauge rotation[26] acts on ψ as

$$\psi \to (1 + i\theta^a \tilde{\sigma}^a)\psi \tag{A10}$$

where $\tilde{\sigma}^a$ are Pauli matrices in the $\pm$ space. This gauge rotation acts on z as

$$\phi_\ell \to \left(1 + i\theta^a T_{\ell m}^a\right)\phi_m, \tag{A11}$$

where the indices $\ell, m = 1 \ldots 4$ and T^a are the antisymmetric Hermitian matrices

$$T^x = \sigma^y \rho^x \quad , \quad T^y = -\sigma^y \rho^z \quad , \quad T^z = \rho^y. \tag{A12}$$

The physical states on a single site, which are eigenstates of H_0, are

$$
\begin{aligned}
c_\alpha^\dagger |0\rangle &\leftrightarrow \left(z_\alpha^* \psi_+^\dagger - \epsilon_{\alpha\beta} z_\beta \psi_-^\dagger \right) |0\rangle \\
|0\rangle &\leftrightarrow |0\rangle \\
c_\uparrow^\dagger c_\downarrow^\dagger |0\rangle &\leftrightarrow \psi_+^\dagger \psi_-^\dagger |0\rangle
\end{aligned} \tag{A13}
$$

These 4 states have energies $-\mu - U/4$, $-\mu - U/4$, $U/4$, and $U/4 - 2\mu$.

Following Hermele[30], let us write these states in a different manner, using the energy levels of a O(4) quantum rotor. All of the following will work on a single site, and so we will drop the site index. We will equate the states of ϕ to that of a quantum particle moving on S^3 with co-ordinate ϕ. On this space, we introduce the angular momentum operators

$$
\mathcal{S}^a = -i\phi_\ell S_{\ell m}^a \frac{\partial}{\partial \phi_m} \quad , \quad \mathcal{T}^a = -i\phi_\ell T_{\ell m}^a \frac{\partial}{\partial \phi_m}. \tag{A14}
$$

In the fermion sector we have the usual angular momentum

$$
\mathcal{L}^a = \psi_p^\dagger \widetilde{\sigma}_{pp'}^a \psi_{p'} \tag{A15}
$$

Then all the states in Eq. (A13) satisfy

$$
\mathcal{T}^a + \mathcal{L}^a = 0. \tag{A16}
$$

Now consider the following Hamiltonian for the rotor and the fermions

$$
\mathcal{H}_0 = K_1 \mathcal{S}^{a2} + K_2 \mathcal{T}^{a2} + K_3 \psi_p^\dagger \psi_p + K_4 \psi_+^\dagger \psi_-^\dagger \psi_- \psi_+ + K_5 \tag{A17}
$$

For appropriate ranges of the K_i couplings, the low-lying states of this Hamiltonian which obey Eq. (A16) map onto the states of the H_0. The zero rotor-angular momentum states must have 0 or 2 fermions, and these map onto the lower two states in Eq. (A13), yielding

$$
\begin{aligned}
K_5 &= U/4 \\
2K_3 + K_4 + K_5 &= U/4 - 2\mu
\end{aligned} \tag{A18}
$$

There are 4 rotor states with angular momentum 1 and wavefunction $\sim \phi_\ell/|\phi|$. Because of the constraint in Eq. (A16), these states must be paired with states with fermion number 1. There are 2 such states, leading to a total of 8 states. However, the conditions in Eq. (A16) eliminate 6 of these states (there are 3 constraints for each fermion polarization), and so only 2 states remain, as in the Hubbard model. The energy of these states yields

$$
3K_1 + 3K_2 + K_3 + K_5 = -\mu - U/4. \tag{A19}
$$

The K_i constants are over-determined, and in an exact treatment of the constraint in Eq. (A16), the precise choice will not matter. Of course, in mean-field theory, different choices will lead to somewhat different results.

Now, following Hermele[30], we can write Eq. (A17) as a path integral over $\phi_\ell(\tau)$ and $\psi_p(\tau)$ and obtain the Lagrangian

$$
\begin{aligned}
\mathcal{L}_0 &= \frac{1}{4(K_1 + K_2)} \left[(\partial_\tau \phi_\ell - i A_\tau^a T_{\ell m}^a \phi_m)^2 + \Delta^2 \phi_m^2 \right] \\
&+ \psi_p^\dagger \left(\partial_\tau \delta_{pp'} - i A_\tau^a \widetilde{\sigma}_{pp'}^a \right) \psi_{p'} + K_3 \psi_p^\dagger \psi_p + K_4 \psi_+^\dagger \psi_-^\dagger \psi_- \psi_+
\end{aligned}
\tag{A20}
$$

where A_τ^a is the time-component of a SU(2) gauge field which imposes the constraint (A16), and Δ^2 imposes the unit length constraint on z_α. We can also insert the parameterization (2.3) into H_1 and obtain the Lagrangain

$$
\begin{aligned}
\mathcal{L}_1 = -\sum_{i<j} t_{ij} & \left[(z_{i\alpha}^* z_{j\alpha}) \left(\psi_{i+}^\dagger \psi_{j+} + \psi_{j-}^\dagger \psi_{i-} \right) \right. \\
&+ (z_{j\alpha}^* z_{i\alpha}) \left(\psi_{i-}^\dagger \psi_{j-} + \psi_{j+}^\dagger \psi_{i+} \right) \\
&+ (\varepsilon^{\alpha\beta} z_{j\alpha}^* z_{i\beta}^*) \left(\psi_{i+}^\dagger \psi_{j-} - \psi_{j+}^\dagger \psi_{i-} \right) \\
&+ \left. (\varepsilon^{\alpha\beta} z_{i\alpha} z_{j\beta}) \left(\psi_{i-}^\dagger \psi_{j+} - \psi_{j-}^\dagger \psi_{i+} \right) \right]
\end{aligned}
\tag{A21}
$$

There is now a natural mean field theory of $\mathcal{L}_0 + \mathcal{L}_1$ which should yield all 4 phases of Ref. 26. The approximations are:

- Ignore the gauge field A_τ^a.

- Factorize the 4-Fermi term, K_4 into $N^a \psi_p^\dagger \widetilde{\sigma}_{pp'}^a \psi_{p'}$ The field N^a is to be determined self-consistently, and will be site-dependent.

- Factorize $\mathcal{L}_1$ into fermion and boson bilinears, as indicated by the parentheses.

- Phases A and C will also have a ϕ condensate. It should be sufficient to work with $\langle \phi \rangle = 0$ in phases B and D, and determine their boundaries to phases A and C

- Phase D should have $N^a = 0$, and also $\langle z_\alpha^* z_\beta^* \rangle = 0$ and $\langle \psi_+^\dagger \psi_- \rangle = 0$.

- The value of Δ^2 is determined as usual by solving the unit length constraint on z_α.

Appendix B: Square lattice antiferromagnetic in an applied gauge flux

This appendix will carry out a computation similar to that of Section II A using gauge-theoretical formulation in Eq. (2.5). Rather than a slowly varying Néel order $n^a(\mathbf{r})$ as

in Eq. (2.2), this appendix will have a slowly varying gauge potential $\mathbf{A}(\mathbf{r})$. The results here will be connected to those of Section II A via Eq. (2.7). However, a precise quantitative equivalence between Eqs. (2.2) and (2.5) requires inclusion of the last two terms of Eq. (A21) in Eq. (2.5), which we will not account for here. The importance of these omitted terms should be clear from Appendix A of Ref. 27.

Now we expand Eq. (2.5) to first order in A_{ij}, and using Eq. (2.6) we can write $H = H_0 + H_1$ where H_0 has the same form as Eq. (2.9) but with the $\psi_\pm$ fermions

$$H_0 = \sum_{\mathbf{k}} \left(\varepsilon_{\mathbf{k}} \psi^\dagger(\mathbf{k}) \psi(\mathbf{k}) + m \psi^\dagger(\mathbf{k} + \mathbf{Q}) \sigma^z \psi(\mathbf{k}) \right), \tag{B1}$$

while H_1 in Eq. (2.11) is replaced by

$$\begin{aligned} H_1 &= -i \sum_{i<j} t(\mathbf{r}_i - \mathbf{r}_j) A_{ij} \left(\psi_i^\dagger \sigma^z \psi_j - \psi_j^\dagger \sigma^z \psi_i \right) \\ &= \sum_{\mathbf{k},\mathbf{q}} \left[\mathbf{A}(\mathbf{q}) \cdot \frac{\partial \varepsilon_{\mathbf{k}}}{\partial \mathbf{k}} \right] \psi^\dagger(\mathbf{k} + \mathbf{q}/2) \sigma^z \psi(\mathbf{k} - \mathbf{q}/2) + \mathcal{O}(\mathbf{q}^2) \end{aligned} \tag{B2}$$

Note that H_1 does not include the omitted terms represented by the ellipses in Eq. (2.5), which appear as the last two terms in Eq. (A21); this will be significant below.

Now we will use the Kubo formula to determine the response to the applied gauge field in H_1. We will work to linear response order $\mathbf{A}$, and to linear order in $\mathbf{q}$.

We have to carefully define an observable: it should be gauge invariant and spin-rotation invariant. For this reason we look at the response in the following

$$M_{ij} \equiv \psi_i^\dagger e^{i\sigma^z A_{ij}} \psi_j \tag{B3}$$

We want to compute the change in $\langle M_{ij} \rangle$ to linear order in $\mathbf{A}(\mathbf{q})$, and in the limit of small $\mathbf{q}$. In momentum space

$$\begin{aligned} \langle M_{ij} \rangle &= \sum_{\mathbf{k},\mathbf{p}} e^{-i\mathbf{k}\cdot\mathbf{r}_i + i\mathbf{p}\cdot\mathbf{r}_j} \left\langle \psi^\dagger(\mathbf{k}) ; \psi(\mathbf{p}) \right\rangle \\ &+ i \left[\sum_{\mathbf{q}} \mathbf{A}(\mathbf{q}) \cdot (\mathbf{r}_j - \mathbf{r}_i) e^{i\mathbf{q}\cdot(\mathbf{r}_j + \mathbf{r}_i)/2} \right] \left[\sum_{\mathbf{k}} e^{-i\mathbf{k}\cdot(\mathbf{r}_i - \mathbf{r}_j)} e^{i\mathbf{Q}\cdot\mathbf{r}_j} \left\langle \psi^\dagger(\mathbf{k}) \sigma^z \psi(\mathbf{k} + \mathbf{Q}) \right\rangle \right] \end{aligned} \tag{B4}$$

In the second term, we have assumed we are expanding to linear order in $\mathbf{A}$, and so assumed momentum conservation in the fermion bilinear expectation value.

We have to expand the first term to linear order in $\mathbf{A}$, and so we expand the second term

in Eq. (B4) using Wick's theorem.

$$\left\langle \psi^\dagger(\mathbf{k}')\psi(\mathbf{p}) \,;\, \psi^\dagger(\mathbf{k} + \mathbf{q}/2)\sigma^z\psi(\mathbf{k} - \mathbf{q}/2)\right\rangle$$

$$= -2\sum_\omega \left[\delta_{\mathbf{p},\mathbf{k}+\mathbf{Q}+\mathbf{q}/2}\delta_{\mathbf{k}',\mathbf{k}-\mathbf{q}/2}G(\mathbf{k} - \mathbf{q}/2)F(\mathbf{k} + \mathbf{q}/2) \right.$$

$$\left. + \delta_{\mathbf{p},\mathbf{k}+\mathbf{q}/2}\delta_{\mathbf{k}',\mathbf{k}+\mathbf{Q}-\mathbf{q}/2}G(\mathbf{k} + \mathbf{q}/2)F(\mathbf{k} - \mathbf{q}/2) \right]. \tag{B5}$$

Also from Eq. (2.14)

$$\left\langle \psi^\dagger(\mathbf{k})\sigma^z\psi(\mathbf{k} + \mathbf{Q})\right\rangle = -2\sum_\omega F(\mathbf{k}) \tag{B6}$$

Putting everything together

$$\delta\langle M_{ij}\rangle = 2\sum_{\mathbf{k},\mathbf{q},\omega} e^{-i\mathbf{k}\cdot(\mathbf{r}_i-\mathbf{r}_j)}e^{i\mathbf{q}\cdot(\mathbf{r}_j+\mathbf{r}_i)/2}e^{i\mathbf{Q}\cdot\mathbf{r}_j}\mathbf{A}(\mathbf{q}) \cdot \left[\vphantom{\frac{\partial}{\partial}} \right.$$

$$\left. \frac{\partial\varepsilon_{\mathbf{k}}}{\partial\mathbf{k}}G(\mathbf{k} - \mathbf{q}/2)F(\mathbf{k} + \mathbf{q}/2) + \frac{\partial\varepsilon_{\mathbf{k}+\mathbf{Q}}}{\partial\mathbf{k}}G(\mathbf{k} + \mathbf{Q} + \mathbf{q}/2)F(\mathbf{k} - \mathbf{q}/2) + \frac{\partial F(\mathbf{k})}{\partial\mathbf{k}} \right] \tag{B7}$$

Explicit evaluation shows that the expression in the square brackets does indeed vanish at $\mathbf{q} = 0$, as is required by gauge invariance. Now expand Eq. (B7) to first order in $\mathbf{q}$ and find

$$\delta\langle M_{ij}\rangle = 2\sum_{\mathbf{k},\mathbf{q}} e^{-i\mathbf{k}\cdot(\mathbf{r}_i-\mathbf{r}_j)}e^{i\mathbf{q}\cdot(\mathbf{r}_j+\mathbf{r}_i)/2}e^{i\mathbf{Q}\cdot\mathbf{r}_j}\mathbf{A}(\mathbf{q}) \cdot \mathbf{I}(\mathbf{k},\mathbf{q}) \tag{B8}$$

where

$$\mathbf{I}(\mathbf{k},\mathbf{q}) = \left[\frac{\partial\varepsilon_{\mathbf{k}}}{\partial\mathbf{k}}\left(\mathbf{q}\cdot\frac{\partial\varepsilon_{\mathbf{k}+\mathbf{Q}}}{\partial\mathbf{k}}\right) - \frac{\partial\varepsilon_{\mathbf{k}+\mathbf{Q}}}{\partial\mathbf{k}}\left(\mathbf{q}\cdot\frac{\partial\varepsilon_{\mathbf{k}}}{\partial\mathbf{k}}\right) \right] \sum_\omega \frac{m/2}{(-i\omega + E_{1\mathbf{k}})^2(-i\omega + E_{2\mathbf{k}})^2} \tag{B9}$$

Combining (B8) and (B9), we have the result analogous to Eq. (2.22):

$$\left\langle c^\dagger(\mathbf{k})c(\mathbf{k} + \mathbf{Q})\right\rangle = -2i\widetilde{\mathcal{F}}(\mathbf{k})\left(\partial_x A_y - \partial_y A_x\right) \tag{B10}$$

where

$$\widetilde{\mathcal{F}}(\mathbf{k}) = \left(\frac{\partial\varepsilon_{\mathbf{k}+\mathbf{Q}}}{\partial\mathbf{k}} \times \frac{\partial\varepsilon_{\mathbf{k}}}{\partial\mathbf{k}}\right)\sum_\omega \frac{m/4}{(-i\omega + E_{1\mathbf{k}})^2(-i\omega + E_{2\mathbf{k}})^2}$$

$$= \frac{m}{2}\left(\frac{\partial\varepsilon_{\mathbf{k}+\mathbf{Q}}}{\partial\mathbf{k}} \times \frac{\partial\varepsilon_{\mathbf{k}}}{\partial\mathbf{k}}\right)\frac{(\text{sgn}(E_{1\mathbf{k}}) - \text{sgn}(E_{2\mathbf{k}}))}{(E_{1\mathbf{k}} - E_{2\mathbf{k}})^3}. \tag{B11}$$

We have written Eq. (B10) in terms of the original electron operators $c(\mathbf{k})$: we are working to linear order in $\mathbf{A}$, and so this order all variables can be mapped onto the original gauge-

invariant operators. Comparing Eq. (B11) with Eq. (2.23), and using Eq. (2.7), we should expect equality between $\mathcal{F}(\mathbf{k})$ and $\widetilde{\mathcal{F}}(\mathbf{k})$. However, while both functions have an identical symmetry structure, and similar singularities at possible Fermi surfaces (which is all we need), they are not precisely equal. This can be traced to the absence of precise equality between Eqs. (2.2) and (2.5), due to the omission of the last two terms in Eq. (A21), which were also important in previous computations[27].

---

[1] *Geometric Phases in Physics*, A. Shapere and F. Wilczek, Eds., Advanced Series in Mathematical Physics, Vol 5, World Scientific, Singapore (1988).

[2] S. Chakravarty, B. I. Halperin, and D. R. Nelson, Phys. Rev. B **39**, 2344-2371 (1989).

[3] F. D. M. Haldane, Phys. Rev. Lett. **61**, 1029 (1988).

[4] N. Read and S. Sachdev, Phys. Rev. Lett. **62**, 1694 (1989).

[5] N. Read and S. Sachdev, Phys. Rev. B **42**, 4568 (1990).

[6] D. Rokhsar and S. A. Kivelson, Phys. Rev. Lett. **61**, 2376 (1988).

[7] S. Sachdev and R. Jalabert, Mod. Phys. Lett. B **4**, 1043 (1990).

[8] T. Senthil, A. Vishwanath, L. Balents, S. Sachdev, and M. P. A. Fisher, Science **303**, 1490 (2004).

[9] T. Senthil, L. Balents, S. Sachdev, A. Vishwanath, and M. P. A. Fisher, Phys. Rev. B **70**, 144407 (2004).

[10] A. W. Sandvik, Phys. Rev. Lett. **98**, 227202 (2007).

[11] R. G. Melko and R. K. Kaul, Phys. Rev. Lett. **100**, 017203 (2008).

[12] F.-J. Jiang, M. Nyfeler, S. Chandrasekharan, and U.-J. Wiese, Stat. Mech. (2008) P02009.

[13] A. B. Kuklov, M. Matsumoto, N. V. Prokof'ev, B. V. Svistunov, and M. Troyer, Phys. Rev. Lett. **101**, 050405 (2008).

[14] O. I. Motrunich and A. Vishwanath, arXiv:0805.1494.

[15] Jie Lou, A. W. Sandvik, and N. Kawashima, Phys. Rev. B **80**, 180414 (2009).

[16] A. W. Sandvik, Phys. Rev. Lett. **104**, 177201 (2010).

[17] A. Banerjee, K. Damle, and F. Alet, arXiv:1002.1375.

[18] A. Tanaka and X. Hu, Phys. Rev. Lett. **95**, 036402 (2005).

[19] A. G. Abanov and P. B. Wiegmann, Nucl. Phys. B **570**, 685 (2000).

[20] T. Senthil and M. P. A. Fisher, Phys. Rev. B **74**, 064405 (2006).

[21] S. Sachdev and S.-C. Zhang, Science **295**, 452 (2002).

[22] T. Grover and T. Senthil, Phys. Rev. Lett. **100**, 156804 (2008).

[23] Hong Yao and Dung-Hai Lee, arXiv:1003.2230.

[24] Xiao-Liang Qi, T. L. Hughes, and Shou-Cheng Zhang **78**, 195424 (2008).

[25] D. J. Thouless, M. Kohmoto, M. P. Nightingale, and M. den Nijs, Phys. Rev. Lett. **49**, 405 (1982).

[26] S. Sachdev, M. A. Metlitski, Yang Qi, and Cenke Xu, Phys. Rev. B **80**, 155129 (2009).

[27] Yang Qi and S. Sachdev, Phys. Rev. B **81**, 115129 (2010).

[28] A. M. Polyakov, Phys. Lett. B **59**, 82 (1975).

[29] R. K. Kaul, M. A. Metlitski, S. Sachdev and C. Xu, Phys. Rev. B **78**, 045110 (2008).

[30] M. Hermele, Phys. Rev. B **76**, 035125 (2007).